

Hybrid simplicial-randomized approximate stochastic dynamic programming for multireservoir optimization

Luckny Zephyr (✉ lzephyr@laurentian.ca)

Laurentian University

Bernard F. Lamond

Université Laval

Pascal Lang

Université Laval

Research Article

Keywords: Reservoir optimization, stochastic dynamic programming, simplicial-randomized approximation, piecewise linear approximation

Posted Date: December 28th, 2023

DOI: <https://doi.org/10.21203/rs.3.rs-3765572/v1>

License:  This work is licensed under a Creative Commons Attribution 4.0 International License.

[Read Full License](#)

Additional Declarations: No competing interests reported.

Hybrid simplicial-randomized approximate stochastic dynamic programming for multireservoir optimization

Luckny Zephyr* Bernard F. Lamond† Pascal Lang‡

December 17, 2023

Abstract

We revisit an approximate stochastic dynamic programming method that we proposed earlier for the optimization of multireservoir problems. The method exploits the convexity properties of the value function to sample the reservoir level space based on the local curvature of the value function, which is estimated by the difference between a lower and an upper bounds (error bound). Unlike the previous approach where the state space was exhaustively partitioned into full dimensional simplices whose vertices formed a discrete grid over which the value function was approximated, here we propose instead a new randomized approach for selecting the grid points from a small number of randomly sampled simplices from which an error bound is estimated. Results of numerical experiments on three literature test problems and simulated midterm reservoir optimization problems illustrate the advantages of the randomized approach which can solve models of higher dimensions than with the exhaustive approach.

Key Words: Reservoir optimization; stochastic dynamic programming; simplicial-randomized approximation; piecewise linear approximation

*Faculty of Management, Laurentian University, Sudbury (Ontario), Canada P3E 2C6. Email: LZephyr@laurentienne.ca.

†Département Opérations et systèmes de décision, Université Laval, Québec (Québec), Canada G1V 0A6. Email: Bernard.Lamond@fsa.ulaval.ca.

‡Département Opérations et systèmes de décision, Université Laval, Québec (Québec), Canada G1V 0A6. Email: pascal.lang.1@ulaval.ca.

1 Introduction

This work deals with a mid-term reservoir optimization problem over a finite planning horizon. In each period, water must be released from the reservoirs to produce electricity. However, these decisions are constrained by not only the availability of water, but also the physical limits of the turbines, and bounds on the level of the reservoirs, that may be set by legal requirements. This problem is rightfully acknowledged to be difficult, in particular due to the uncertainty associated with the natural inflows to the reservoirs, e.g., snow-melt, snow water equivalent.

Thus, mid-term reservoir optimization is inherently a multiperiod stochastic problem. As a result, the problem is often cast as a multiperiod stochastic program or formulated under the framework of stochastic dynamic programming. Numerous meta-heuristic approaches have also been proposed for reservoir optimization problems, e.g., [3]. Two recent systematic reviews of such methods are available in [4, 5].

When stochastic programming is employed to solve the problem, the random variables, e.g., natural inflows, and demand for energy, are discretized via a so-called scenario tree, which easily becomes intractable if a detailed representation of the stochastic variables is needed. This issue is often dealt with through decomposition strategies, such as Benders' decomposition, e.g., [10, 52], the progressive hedging algorithm, e.g., [28, 9, 62], in which the so-called non-anticipativity constraints are dualized in the objective function, stochastic dynamic programming (SDP) [53, 55], scenario tree reduction strategies [23, 59], model predictive control, e.g., [44, 57, 43], etc.

Being a sequential decision-making problem, the mid-term optimization of reservoir lends itself naturally to stochastic dynamic programming (SDP). Indeed, in the groundbreaking theory of dynamic programming presented in [6], Bellman decomposed a *multi-stage decision process* stagewise in a coordinated manner. Thus, it is no surprise that DP quickly found a fertile ground for reservoir optimization applications [35].

The solution of SP or SDP reservoir management problems broadly consists of two main steps, namely (i) the calculation of an expectation; and (ii) an optimization step, or vice-versa. In models for the mid- or long-term planning of hydroelectric production, the opti-

49 mization step often has to deal with nonlinear objective functions, due to, among others,
50 nonlinear production functions [11]. To take advantage of the widespread availability of lin-
51 ear programming solvers, the combined power response curve of the turbines at a power plant
52 can often be approximated reasonably well by a concave, piecewise linear function of tur-
53 bined water flow, even though the response curves of the individual turbines may be highly
54 nonlinear. For instance, this strategy is used by companies like Hydro-Quebec [9] and Rio
55 Tinto [19] (4-reservoir system) to approximate production functions; similarly in studies on
56 the Colombian power network [40] (15-reservoir system), on a “network of hydropower plants
57 and irrigated areas in the Nile Basin” [29], a network of power plants in southern Brazil [8]
58 (4-reservoir system). An immediate consequence of this approximation scheme is that under
59 mild assumptions on the terminal value/cost-to-go function, one can easily show that the
60 value/cost-to-go functions are concave/convex in the reservoir levels. These ideas are also
61 exploited in [63, 64, 65] where an approximate stochastic dynamic programming model of
62 a multiperiod, multireservoir hydroelectric system is presented in which the Bellman value
63 function is approximated by a piecewise linear function that is evaluated by linear program-
64 ming. The piecewise linear approximation is supported by a finite grid of node points (or
65 vertices) in the continuous state space where the Bellman function is evaluated at the nodes.
66 For other states, the value function is approximated by the best linear interpolation between
67 nodes.

68 Resorting to SDP to solve reservoir optimization problems poses another technical chal-
69 lenge, since in theory an optimization problem has to be solved for each possible state value,
70 which is impossible due to the fact that the reservoir level space is continuous. Thus, the
71 latter must be discretized or sampled.

72 The simplest discretization strategy to approximate our continuous dynamic program
73 consists in constructing a uniform grid, obtained as the Cartesian product of same-size and
74 fixed-spacing grids along each dimension of the reservoir level (state) space. However, this
75 approach is impractical, as the complexity of the problem increases exponentially with the
76 dimension of the state space, limiting applications to three to four reservoirs. This is known
77 in dynamic programming as the *curse of dimensionality*.

78 The above uniform discretization scheme has inspired the development of parsimonious

79 approaches that select sub-samples of points along each dimension of the state space, and
80 then use analytical functions based on multi-linear interpolations, polynomials, cubic splines,
81 to approximate the Bellman function [33]. As these techniques did not prove to be a panacea
82 against the dimensionality issue, statistical techniques have been employed to sample the
83 state space more efficiently. Perhaps, one of the oldest strategies is *Latin hypercube*, in
84 which each dimension of the state space is discretized into p values, and the overall sample
85 is chosen so that each uni-dimensional value is selected exactly once. This is a special case
86 of *orthogonal array with strength d* , where $d \leq n$, n being the dimension of the state space.
87 Under this scheme, each uni-dimensional grid point is chosen exactly a same number of times
88 in each possible d -dimensional subspace [16].

89 Other sampling techniques resort to some form of Monte Carlo simulation to sample the
90 state space in contrast to the discretization strategies used in the above-mentioned schemes.
91 For instance, in stochastic dual dynamic programming (SDDP), originally developed for
92 reservoir optimization problems in the seminal works [49, 47, 48], the connections between
93 SP and SDP, e.g., [53, 55], are exploited to efficiently sample the reservoir level space, based
94 on Monte Carlo simulation. Assuming the natural inflows to be temporally independent,
95 SDDP alternates between a backward pass, to build the so-called *value/cost-to-go functions*,
96 and a forward step, to draw a sample of state space values to approximate the value/cost-
97 to-go functions in the next backward loop, until a convergence criterion is met.

98 On the other hand, quasi-randomized or quasi-Monte Carlo sampling techniques, where
99 randomly generated points are replaced with more evenly distributed ones, based on the
100 notion of *low-discrepancy sequences*, are known to enjoy faster convergence rate than ran-
101 domized techniques [13, 14]. For further account of reservoir optimization techniques, please
102 see [35, 50, 1, 22].

103 In [63, 64, 65], we proposed an approximate SDP approach for the mid-term optimization
104 of reservoirs. The iterative scheme amounts to partitioning the reservoir level space into a
105 finite but potentially large set of simplices in each period of the planning horizon. The
106 value function is evaluated at the extreme points of the resulting simplices, and interpolated
107 elsewhere. In addition, error bounds are computed for all simplices and, at each iteration,
108 a new grid point associated with largest error bound is added to the grid, and the simplex

109 containing the point is divided into smaller simplices that are appended to the list of existing
110 simplices. Thus, in each period, constructing the grid requires to maintain a complete list
111 of simplices that spans the whole reservoir level space. Because the number of simplices
112 increases fast with the grid size and with the dimension of the state space, this method
113 becomes impractical for models with many reservoirs.

114 This work is essentially a revisit of the sampling approach presented in [63, 64, 65], in
115 which, in each period, we avoid making a list of simplices and randomly sample the reservoir
116 level space to select grid points at which the value function is approximated. We resort
117 to linear programming to identify the simplex containing a candidate grid point and to
118 obtain a local error bound on the approximation of the Bellman function. Then, the global
119 error bound is estimated using a statistical model. This is motivated by the computational
120 burden of the simplicial scheme, induced by the exponential growth of the number of created
121 simplices, which limits applications to dimensions lower than ten, based on our empirical
122 observations.

123 The remainder of the paper is organized as follows. We provide a detailed description
124 of the problem under analysis in Section 2. Next, we discuss a simplicial approximate
125 stochastic dynamic programming (ASDP) scheme for the problem in Section 3, followed by
126 a hybrid Monte Carlo simplicial ASDP proposal in Section 4. Results of extensive numerical
127 experiments are reported in Section 5. The paper ends with concluding remarks in Section
128 6.

129 **2 Reservoir optimization problem**

130 A hydropower system often comprises power plants that may or may not be associated
131 with reservoirs. Reservoir optimization problems are typically divided into long-, mid-, and
132 short-term, depending on, among other factors, the length of the planning horizon [51]. In
133 a mid-term problem, which is of interest to us, the time span is typically between one and
134 five years [58], divided into daily, weekly, or monthly time steps [65].

135 In this work, we consider a mid-term reservoir optimization problem over a finite horizon
136 of T periods. At each period t , the operator of the system wants to find the release, \mathbf{u}_t , and

137 storage, \mathbf{s}_t , decisions that maximize the expected total energy production. Without loss of
 138 generality, we assume each plant to be associated with a reservoir, and the random natural
 139 inflows to the reservoirs are denoted $\tilde{\mathbf{q}}_t$.

140 At each period t , water released from each reservoir $i = 1, \dots, n$, is limited by the
 141 turbine capacity, $\bar{\mathbf{u}}$, to prevent physical damage. Similarly, due to legal and environmental
 142 considerations, at each time period, the level of the reservoirs must be kept between lower
 143 and upper limits, $\underline{\mathbf{s}}$, and $\bar{\mathbf{s}}$, respectively.

144 In addition, we assume the topology of the system to form an arborescence, i.e., a com-
 145 bination of reservoirs in series and in parallel. Water released upstream are absorbed by
 146 the immediate successors (reservoirs) at the same period, and in case of overflow, excess of
 147 water from upstream reservoirs, \mathbf{y}_t , are absorbed by immediate successors or spilled out of
 148 the system.

149 At each period t , the state of the system is governed by the standard mass balance
 150 equation:

$$\mathbf{s}_t = \mathbf{s}_{t-1} - \mathbf{B}\mathbf{u}_t - \mathbf{C}\mathbf{y}_t + \tilde{\mathbf{q}}_t, \quad (1)$$

151 where entries of the square connectivity matrix, B_{ij} , are 1 for $i = j$, -1 if the water released
 152 from reservoir j is routed to reservoir i , and 0, otherwise. The elements of the square matrix
 153 \mathbf{C} similarly define the routing of the spilled water.

154 As in [63], for each plant $i = 1, \dots, n$, we assume the production function p_{it} to nonlin-
 155 early depend on the release and the storage at the beginning of the period.

A typical multi-period mid-term reservoir optimization problem reads:

$$\max_{\mathbf{u}_t, \mathbf{y}_t} \mathbb{E}_{\tilde{\mathbf{q}}_t} \left[\sum_{t=1}^T \sum_{i=1}^n p_{it}(u_{it}) + V_{T+1}(\mathbf{s}_{T+1}) \right] \quad (2)$$

$$\text{s.t., for } t = 1, \dots, T : \quad (3)$$

$$\mathbf{s}_{t+1} = \mathbf{s}_t - \mathbf{B}\mathbf{u}_t - \mathbf{C}\mathbf{y}_t + \tilde{\mathbf{q}}_t \quad (4)$$

$$\underline{\mathbf{s}} \leq \mathbf{s}_{t+1} \leq \bar{\mathbf{s}} \quad (5)$$

$$0 \leq \mathbf{u}_t \leq \bar{\mathbf{u}} \quad (6)$$

$$\mathbf{y}_t \geq \mathbf{0}, \quad (7)$$

156 where, \mathbb{E} is the expectation operator, and $V_{T+1}(\mathbf{s}_{T+1})$, assumed to be a concave function,

157 captures the terminal value of the stored water in the system.

At each time period t , assume the operator of the system observes the level of the reservoirs, the realization \mathbf{q}_t of the random natural inflows, $\tilde{\mathbf{q}}_t$, and decides on the water released, spilled and stored to find the best trade-off between utilizing the available water for current production needs and leaving it for the future. Under this setting, and by Bellman's principle of optimality, Problem (2)-(7) can be reformulated as a sequence of coordinated subproblems, moving backward in time, i.e., for $t = T, T - 1, \dots, 1$,

$$V_t(\mathbf{s}_t, \mathbf{q}_t) := \max_{\mathbf{u}_t, \mathbf{y}_t} \left\{ \sum_{i=1}^n p_{it}(u_{it}) + \mathcal{V}_{t+1}(\mathbf{s}_{t+1}, \tilde{\mathbf{q}}_{t+1}) \right\} \quad (8)$$

$$\text{s.t. (4) - (7),} \quad (9)$$

158 where $V_t(\cdot)$, called value function, measures the value of the stored water from period t
 159 onward, and $\mathcal{V}_{t+1}(\cdot) := \mathbb{E}_{\tilde{\mathbf{q}}_{t+1}|\mathbf{q}_t} V_{t+1}(\mathbf{s}_{T+1}, \tilde{\mathbf{q}}_{t+1})$. As in [63, 64, 65], since the terminal value
 160 function is concave, we observe that if the production functions are concave, the problem is
 161 convex and the concavity of the value function $V_t(\mathbf{s}_t, \cdot)$ propagates backwards.

162 **Proposition 1.** *If (i) $p_{it}(u_{it})$ is concave in u_{it} , and (ii) the support of $\tilde{\mathbf{q}}_t$ is discrete and*
 163 *finite, then $V_t(\mathbf{s}_t, \cdot)$ is concave in \mathbf{s}_t .*

164 *Proof.* The feasible domain of Problem (8)-(9) is a polyhedron; since $V_{T+1}(\mathbf{s}_{T+1}, \cdot)$ is concave
 165 in \mathbf{s}_{T+1} , by the concavity of the production function, and the linearity property of the
 166 expectation operator, it follows that $V_T(\mathbf{s}_T, \cdot)$ is concave in \mathbf{s}_T . The concavity property then
 167 follows by backward induction on t , for $t = T - 1, \dots, 1$. \square

168 Problem(8)-(9) may be nonlinear, in particular due to the nonlinearity of the production
 169 functions. Indeed, in practice, production functions are often nonconcave (i) due to head
 170 effects, i.e, the difference between upstream and downstream reservoir levels; and (ii) because
 171 the power produced by a plant varies nonlinearly with the water release and the number of
 172 turbines, whose efficiency may decrease beyond a maximum flow rate [65]. In industry, this
 173 issue is often dealt with by approximating production functions with their concave envelopes
 174 (e.g., [29, 9, 19, 40]).

As in [64, 65], the nonlinearity hurdle is passed using inner generalized linear programming (GLP) on a support grid to obtain a convex approximation of the problem. For each plant i , assume that the production function is evaluated over a finite grid of reservoir releases $\mathcal{U}_t := \{u_i^k | k \in K_i\}$, constructed in a preprocessing step, where K_i is the set of indices associated with the discrete releases u_i^k , $i = 1, \dots, n$. Similarly, the expected value function $\mathcal{V}_{t+1}(\cdot)$ is evaluated over a finite set of states $\mathcal{G}_t := \{\mathbf{s}_{t+1}^j | j \in J_t\}$, where J_t is the set of indices associated with the discrete storage vectors \mathbf{s}_{t+1}^j , possibly obtained by division of simplices as explained in Section 3. The following GLP is a linear approximation of Problem (8)-(9):

$$\hat{V}_t(\mathbf{s}_t, \mathbf{q}_t) := \max_{\mathbf{u}_t, \mathbf{y}_t, \boldsymbol{\lambda}, \boldsymbol{\mu}} \left\{ \sum_{i=1}^n \sum_{k \in K_i} p_{it}(u_i^k) \lambda_i^k + \sum_{j \in J_t} \hat{\mathcal{V}}_{t+1}(\mathbf{s}_{t+1}^j, \cdot) \mu^j \right\} \quad (10)$$

$$\text{s.t. (4) - (7)} \quad (11)$$

$$u_{it} - \sum_{k \in K_i} \lambda_i^k u_i^k = 0, \quad i = 1, \dots, n \quad (12)$$

$$\mathbf{s}_{t+1} - \sum_{j \in J_t} \mu_j \mathbf{s}_{t+1}^j = 0 \quad (13)$$

$$\sum_{k \in K_i} \lambda_i^k = 1, \quad i = 1, \dots, n \quad (14)$$

$$\sum_{j \in J_t} \mu^j = 1 \quad (15)$$

$$\boldsymbol{\lambda}, \boldsymbol{\mu} \geq 0 \quad (16)$$

175 Note that $\boldsymbol{\lambda}$ and $\boldsymbol{\mu}$ are vectors of convex combination coefficients, as expressed in equations
 176 (12)-(16). Thus, for each power plant i , in each period, the release is interpolated on the
 177 discrete release values; similarly the next period storage level is interpolated on the storage
 178 grid.

179 Since the calculation of the expected value is not the focus of this work, we assume the
 180 natural inflow process to be finite, and serially independent. As a result, in the numerical
 181 experiments, in each period, we will use Monte Carlo simulation to generate a finite sample
 182 of natural inflows, and the expected value of the approximate value function, $\hat{\mathcal{V}}_{t+1}(\cdot)$, will
 183 be estimated by the sample mean of the $\hat{V}_{t+1}(\mathbf{s}_t, \mathbf{q}_t)$'s. Similarly, at each time period, for
 184 a given state point \mathbf{s}_t^k , let $\boldsymbol{\pi}_t^j$ be a vector of optimal dual prices associated with the mass-
 185 balance constraints (1), for a given observation $\mathbf{q}_t^j, j = 1, \dots, J$. In the sequel, a vector of

186 subgradient, \mathbf{g}_t^j , will be taken as the sample mean of the $\boldsymbol{\pi}_t^j$'s.

187 In closing this section, observe that since (i) Problem (10)-(16) is linear and its objective
188 maximized; and (ii) s_t is in the right hand side of the water-balance constraint (4), therefore
189 the GLP is a parametric linear program, so that its optimal value function $\hat{V}_t(\mathbf{s}_t, \mathbf{q}_t)$ is a
190 piecewise linear concave function of \mathbf{s}_t .

191 **3 Simplicial approximate stochastic dynamic program-** 192 **ming**

193 Despite its theoretical elegance, it is well known that dynamic programming is plagued by
194 the so-called *curse of dimensionality*, in the sense that the computational burden of Problem
195 (10)-(16) increases exponentially with the dimension, n , of the reservoir level space S_t , except
196 for rare cases (e.g., unconstrained linear systems with quadratic production functions), for
197 which analytical solutions can be derived easily. As a result, the problem cannot be solved
198 for all possible reservoir level vectors; thus, we have to resort to some numerical procedure.
199 To tackle the curse of dimensionality, in each time period t , we need to select a sample of
200 discrete state vectors $\mathcal{G}_t := \{\mathbf{s}_t^j \in S_t, j = 1, 2, \dots, m\}$, $t = T, T-1, \dots, 1$. As discussed earlier,
201 popular sampling techniques include Monte Carlo simulation [17, 40, 61, 39, 21], quasi-Monte
202 Carlo simulation [13, 2, 31], Latin hypercube [25, 31], orthogonal arrays [24, 15].

203 The sampling approach presented in [63, 65, 64], that we revisit in this work, exploits the
204 concavity property of the value function in each period to iteratively sample the state space
205 based on the curvature of the value function, which is estimated by the difference between
206 an upper and a lower bounds. This is the focus of the next two subsections.

207 **3.1 Simplicial sampling of the reservoir level space**

208 Our state space is defined by the level of the reservoirs, which is confined within the hyper-
209 rectangle $S_t := \{\mathbf{s}_t \in \mathbb{R}^n \mid \underline{\mathbf{s}} \leq \mathbf{s}_t \leq \bar{\mathbf{s}}\}$, as defined by the box constraint (5). As a result, the
210 state space is continuous, and as aforementioned, the approximate value function (10)-(16)
211 cannot be evaluated for all possible pairs $(\mathbf{s}_t, \mathbf{q}_t)$. Therefore, we have to resort to some form

212 of discretization or sampling of the state space S_t .

213 Under a simplicial approximate stochastic dynamic scheme, the set S_t is iteratively par-
 214 titioned into smaller *convex* subsets, called *simplices*, and the approximate value function
 215 (10)-(16) is evaluated at their vertices, or extreme points.

216 Simplicial partitioning of convex sets is widespread in the global optimization literature
 217 (e.g., [27, 66, 46, 45, 32, 56, 7]), and less popular in the field of dynamic programming (e.g.,
 218 [65, 64, 63, 30, 60, 54]). Perhaps simplicial partitioning has received a lot of attention in
 219 global optimization as a simplex is an n -dimensional polyhedron with “the minimal number
 220 of vertices”, at which the function is evaluated [45]. More formally,

221 **Definition 1.** Let S be some set in the Euclidean space \mathbb{R}^n , its affine envelope is the set of
 222 all affine combinations of points in S , or equivalently the smallest affine set that contains S ,
 223 i.e., the set $\mathbf{aff} S := \left\{ \sum_{i=1}^k \lambda_i x^i \mid x^i \in S, i = 1, \dots, k, \sum_{i=1}^k \lambda_i = 1 \right\}$; its convex envelope is
 224 the set of all convex combinations of points in S , or equivalently, the smallest convex set that
 225 contains S , i.e., the set $\mathbf{conv} S := \left\{ \sum_{i=1}^k \lambda_i x^i \mid x^i \in S, \lambda_i \geq 0, i = 1, \dots, k, \sum_{i=1}^k \lambda_i = 1 \right\}$.

226 Furthermore,

227 **Definition 2.** A closed convex set $\mathcal{B} \in \mathbb{R}^n$ is called a simplex if it is the convex envelope of
 228 $n + 1$ affinely independent points $\mathbf{s}^1, \mathbf{s}^2, \dots, \mathbf{s}^{n+1}$ in \mathbb{R}^n , i.e., $\mathcal{B} := \mathbf{conv} \{ \mathbf{s}^1, \dots, \mathbf{s}^{n+1} \} :=$
 229 $\left\{ \sum_{i=1}^{n+1} \lambda_i \mathbf{s}^i \mid \lambda_i \geq 0, i = 1, \dots, n + 1, \sum_{i=1}^{n+1} \lambda_i = 1 \right\}$.

230 As examples, a one-dimensional simplex is a line segment, a two-dimensional simplex a
 231 triangle, and a three-dimensional simplex a tetrahedron.

232 Partitioning the hyperrectangular state set S_t into simplices entails two steps, namely, (i)
 233 its initial partitioning into simplices; and (ii) the iterative subdivision of existing simplices
 234 until a prescribed criterion is met. The popular *Kuhn triangulation*, implemented in this
 235 work for our benchmark method, partitions S_t into $n!$ initial simplices [37, 41]. By a simple
 236 change of scale, each point $\mathbf{s}_t \in S_t$ can be mapped to a point $\mathbf{0} \leq \mathbf{x}_t \leq \mathbf{e}$; \mathbf{e} being an n -vector
 237 filled with 1’s. Then each simplex in the Kuhn triangulation corresponds to one possible
 238 permutation, p , of the indices $(1, \dots, n)$ of the dimension of \mathbf{x}_t , and is given by the set of
 239 points \mathbf{x}_t whose coordinates satisfy the inequalities $0 \leq x_t^{p(1)} \leq x_t^{p(2)} \leq \dots \leq x_t^{p(n)} \leq 1$ [20].

240 A less expensive strategy, called *Delaunay triangulation*, partitions a hyperrectangle into
 241 at most $\mathcal{O}(N^{\lceil \frac{n}{2} \rceil})$ simplices, where $N = 2^n$ [66]. In [63, 64], starting with its 1-dimensional
 242 faces (line segments), k -dimensional faces of the hyperrectangle are iteratively lifted into
 243 $k + 1$ -dimensional simplices until the hyperrectangle is partitioned into n -dimensional sim-
 244 plices. The complexity of this proposal is more than exponential in the dimension n of the
 245 hyperrectangle.

246 If either the Kuhn or the Delaunay triangulation is used, the initial step generates a grid
 247 of 2^n points, i.e., the vertices of the hyperrectangle, at which the approximate value function
 248 (10)-(16) is evaluated. If one wants to densify the initial grid in the hope of improving
 249 the approximation, the initial simplices can iteratively be subdivided into smaller ones. A
 250 popular technique used in global optimization consists in bisecting edges of simplices based on
 251 their diameter or local Lipschitz lower bounds (e.g., [66, 46]). Another population strategy,
 252 called radial or ω -subdivision [66], consists in choosing a point in some d -dimensional
 253 subset of a simplex \mathcal{B} , $d = 1, \dots, n - 1$, called a *face* of \mathcal{B} , and creating subsimplices around
 254 this point (e.g., [32, 56, 7, 63, 64, 65]).

255 More specifically, let $\mathcal{B} \subset \mathbb{R}^n$ be an n -dimensional simplex generated by the $n + 1$ affinely
 256 independent points $\{\mathbf{s}^1, \mathbf{s}^2, \dots, \mathbf{s}^{n+1}\}$, and denote $\mathbf{S}_{\mathcal{B}} := [\mathbf{s}^1, \mathbf{s}^2, \dots, \mathbf{s}^{n+1}] \in \mathbb{R}^{n \times (n+1)}$ the full
 257 row rank associated matrix. It follows from Definition 2 that a point \mathbf{s} lives in \mathcal{B} if and only
 258 if the system

$$\begin{bmatrix} \mathbf{S}_{\mathcal{B}} \\ \mathbf{e}^\top \end{bmatrix} \boldsymbol{\lambda} = \begin{pmatrix} \mathbf{s} \\ 1 \end{pmatrix}, \quad \boldsymbol{\lambda} \geq \mathbf{0}, \quad (17)$$

259 has a unique solution $\boldsymbol{\lambda} \in \mathbb{R}^{n+1}$. In addition, let $\mathcal{B}(\mathbf{s})$ be a subset of $\{1, \dots, n + 1\}$ such that
 260 in eq. (17), $\lambda_j > 0$, $j \in \mathcal{B}(\mathbf{s})$. Let $\mathbf{S}_{\mathcal{B}(\mathbf{s})}$ be the $n \times (n + 1)$ matrix obtained by replacing the
 261 j^{th} column of $\mathbf{S}_{\mathcal{B}}$, $j \in \mathcal{B}(\mathbf{s})$, with the point \mathbf{s} , which we assume is not a vertex of the simplex.
 262 Clearly, the columns of $\mathbf{S}_{\mathcal{B}(\mathbf{s})}$ are affinely independent; as a result, their convex envelope
 263 defines a simplex. This way, \mathcal{B} is subdivided into d simplices, d being the cardinality of $\mathcal{B}(\mathbf{s})$.

264 Illustrative examples of simplicial subdivision are provided in Figure 1. In case (i), the
 265 *division point* C is located in the *relative interior* of the simplex $[A, B]$, which is subdivided
 266 into two simplices, namely $[A, C]$ and $[C, B]$. In case (ii), the division point, v , lies in the
 267 relative interior of the simplex $[x, y, z]$; the latter is partitioned into three simplices. Lastly,

268 the simplex $[x', y', z']$ is partitioned into two simplices, since the division point v' is located on
 269 the line segment $[x', y']$.

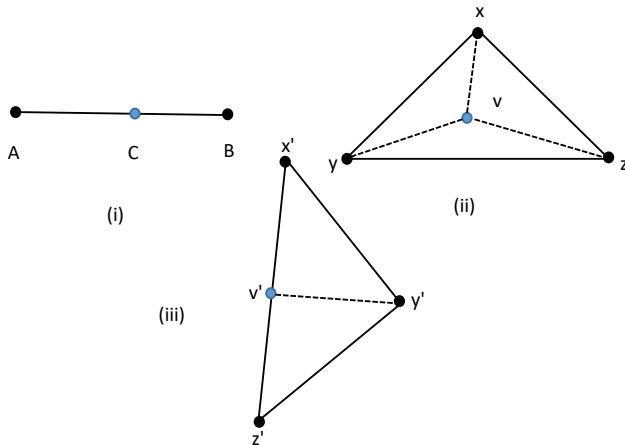


Figure 1: Illustrative examples of simplicial subdivision.

269

270 3.2 Simplicial piecewise linear approximation of the value function

271 In any period t , assume at some iteration of the simplicial algorithm, the state space S_t has
 272 been partitioned into simplices, and the expected value function has been evaluated at the
 273 extreme points $\mathbf{s}_t^k \in S_t$, $k = 1, \dots, K$, $f^k := \hat{V}_t(\mathbf{s}_t^k, \tilde{\mathbf{q}}_t)$. (In the sequel, we drop the time
 274 index t for ease of notation.) Then, for any point $\mathbf{s} \in S$, the expected value function can be
 275 approximated by the following linear program, which by the concavity of the approximate
 276 value function yields a lower bound, $B_L(\mathbf{s})$:

$$B_L(\mathbf{s}) := \max \sum_{k=1, \dots, K} \lambda_k f^k \text{ s.t. } \mathbf{s} = \sum_{k=1, \dots, K} \lambda_k \mathbf{s}^k, \quad \sum_{k=1, \dots, K} \lambda_k = 1, \text{ and } \lambda_k \geq 0 \forall k. \quad (18)$$

277 Let $\mathcal{B}(\mathbf{s})$ be the set of indices of the nonzero components λ_k in a basic optimal solution
 278 of the linear program (18); $\mathcal{B}(\mathbf{s})$ contains at most $n + 1$ elements so that the point \mathbf{s} can
 279 be expressed as a convex combination of at most $n + 1$ vertices, and the set of all convex
 280 combinations of these vertices is a simplex. Also, if vectors of subgradients \mathbf{g}^k , $k \in \mathcal{B}(\mathbf{s})$, are
 281 known at the grid points \mathbf{s}^k , then the expected value function is bounded above by:

$$B_U(\mathbf{s}) := \min_{k \in \mathcal{B}(\mathbf{s})} f^k + \mathbf{g}^{k\top} (\mathbf{s} - \mathbf{s}^k). \quad (19)$$

282 Then $B_L(\mathbf{s}) \leq f(\mathbf{s}) \leq B_U(\mathbf{s})$ so that $B_U(\mathbf{s}) - B_L(\mathbf{s})$ is an upper bound on the approximation
 283 error at the point \mathbf{s} using the support vertices $\mathbf{s}^1, \dots, \mathbf{s}^K$. It is also pointed out in [63] that
 284 the largest error bound on the simplex with vertex set \mathcal{B} is given by the linear program:

$$\begin{aligned} \bar{E}_{\mathcal{B}} &:= \max_{\mathbf{s}, \phi, \lambda_k, k \in \mathcal{B}} \phi - \sum_{k \in \mathcal{B}} \lambda_k f^k \\ \text{s.t. } &\mathbf{s} = \sum_{k \in \mathcal{B}} \lambda_k \mathbf{s}^k, \sum_{k \in \mathcal{B}} \lambda_k = 1, \lambda_k \geq 0 \text{ and } \phi \leq f^k + \mathbf{g}^{k\top}(\mathbf{s} - \mathbf{s}^k), \forall k \in \mathcal{B}. \end{aligned} \quad (20)$$

285 If the error bound $\bar{E}_{\mathcal{B}}$ exceeds a certain criterion, then an optimal point $\mathbf{s}_{\mathcal{B}}^*$ of (20) would
 286 be a candidate vertex for being added to the set of vertices as $\mathbf{s}^{K+1} := \mathbf{s}_{\mathcal{B}}^*$. Similarly, if
 287 there exists some analytical expression for the function $f(\mathbf{s}) := \hat{V}_t(\mathbf{s}_t, \mathbf{q}_t)$, the largest actual
 288 approximation error on a simplex with vertices in \mathcal{B} can be found through the nonlinear
 289 program:

$$E_{\mathcal{B}} := \max_{\mathbf{s}, \lambda_k, k \in \mathcal{B}} f(\mathbf{s}) - \sum_{k \in \mathcal{B}} \lambda_k f^k \text{ s.t. } \mathbf{s} = \sum_{k \in \mathcal{B}} \lambda_k \mathbf{s}^k, \sum_{k \in \mathcal{B}} \lambda_k = 1 \text{ and } \boldsymbol{\lambda} \geq \mathbf{0}. \quad (21)$$

290 In the approach of [63, 64, 65], an initial set of vertices is first chosen, for example the
 291 2^n vertices of the hyperrectangle S plus one interior point $\mathbf{s}^{(2^n+1)}$. Next an initial set of
 292 simplices is explicitly enumerated that spans these vertices. Then the linear program (20) is
 293 solved for every simplex in the set and the next vertex to be added is selected as the optimal
 294 solution $\mathbf{s}_{\mathcal{B}}^*$ for the simplex \mathcal{B} with the largest error bound $\bar{E}_{\mathcal{B}}$. Such a point $\mathbf{s}_{\mathcal{B}}^*$ is called a
 295 division point and the list of simplices is correspondingly updated by deleting the simplex
 296 with vertex set \mathcal{B} from the list and adding to the list the new simplices created by dividing \mathcal{B} .
 297 Iterating this way until a termination criterion is satisfied, the method of [63, 64, 65] stops
 298 with a list of, say, K vertices $\mathbf{s}^1, \dots, \mathbf{s}^K$ at which the approximate value function and its
 299 expectation are evaluated, together with a potentially very large list of associated simplices.

300 The advantage of this scheme is that it provides a monotonic error bound sequence on
 301 the approximation error. However, its Achille's heel is the exhaustive examination of the list
 302 of created simplices that is kept in memory in each time period, and the slow convergence.
 303 Depending on the size of such a list, this might be very expensive in terms of memory usage;
 304 this is the focus of the next subsection.

3.3 Complexity and convergence analysis

A detailed complexity analysis of general operations on simplices (not the simplicial approximation itself) is provided in [65]. In particular, at each iteration k of the procedure, assume we have a list of r^k *active* simplices, finding the simplex with the worst approximation error requires $\mathcal{O}(r^k)$ operations.

Now, assume we want to partition the hypercube S into simplices until a desired error bound, \bar{E}_0 , is attained. Therefore, our goal is to find a full-dimensional simplex $\mathcal{B} \subset S$ generated by the columns of a full row rank matrix $\mathbf{S}_{\mathcal{B}} \in \mathbb{R}^{n \times (n+1)}$, such that the optimal value of (20) is $\bar{E}_{\mathcal{B}} \leq \bar{E}_0$. Toward this end, we first decompose the hypercube S into initial simplices, and for each created simplex solve (20) to find the largest error bound as well as the division point \mathbf{s} . Then, the initial simplex with the largest error is divided at the corresponding division point using the radial ω -subdivision strategy. We repeat the same process until the threshold \bar{E}_0 is met.

Proposition 2. *Let $\text{Vol}(S)$ be the volume of the hyperrectangle S , the number of simplices required to achieve the error bound \bar{E}_0 is of the order $\mathcal{O}\left(\frac{\text{Vol}(S)n!}{(n+1)\bar{E}_0^{n/2}}\right)$.*

A proof of this proposition is provided in Appendix A.

Furthermore,

Proposition 3. *Assume at each iteration of the simplicial scheme, the ω -subdivision of simplex is used, the simplicial algorithm will converge to the desired error bound \bar{E}_0 in a finite number of steps, which is proportional to an exponential factor.*

Proof. Under the ω -subdivision strategy, at each iteration k of the simplicial partitioning scheme, the number of created simplices (subdivision of the simplex with the highest error bound), N^k , is $2 \leq N^k \leq n+1$. In addition, assume K iterations (simplex subdivisions) are performed, and N simplices created, then we have $2K \leq KN^k \leq K(n+1)$, i.e., $K \geq \frac{N}{n+1} \geq \frac{2K}{n+1}$. It follows from (32) that K is of the order $\mathcal{O}\left(\frac{\text{Vol}(S)n!}{\bar{E}_0^{n/2}}\right)$, which concludes the proof. \square

Let us numerically illustrate Proposition (3). First, let us consider hypothetical quadratic expected value functions, of the form $\mathcal{V}(\mathbf{s}) = -\frac{1}{2}\mathbf{s}^\top \mathbf{A}\mathbf{s} + \mathbf{b}^\top \mathbf{s}$, where the matrices \mathbf{A} and vectors \mathbf{b} are randomly generated.

333 Let us consider relative error bounds \overline{E}'_0 , as the ratio of a simplex error bound to the
 334 maximal error over the initial simplices. For each considered state dimension and relative
 335 error threshold indicated in the results reported in Figure 2, five replications of the simplicial
 336 decomposition algorithm are performed.

337 Figure 2 depicts the natural logarithm of the average total number of created simplices
 338 (\overline{N}), grid points (\overline{G}), iterations (\overline{K}), which also is the additional simplices created (in addi-
 339 tion to the initial ones), and the CPU time (\overline{t}), for different error thresholds and state space
 340 dimensions. These results confirm that the computational burden to achieve a fixed error
 341 bound increases more than exponentially with the dimension, n , of the hyperrectangles.

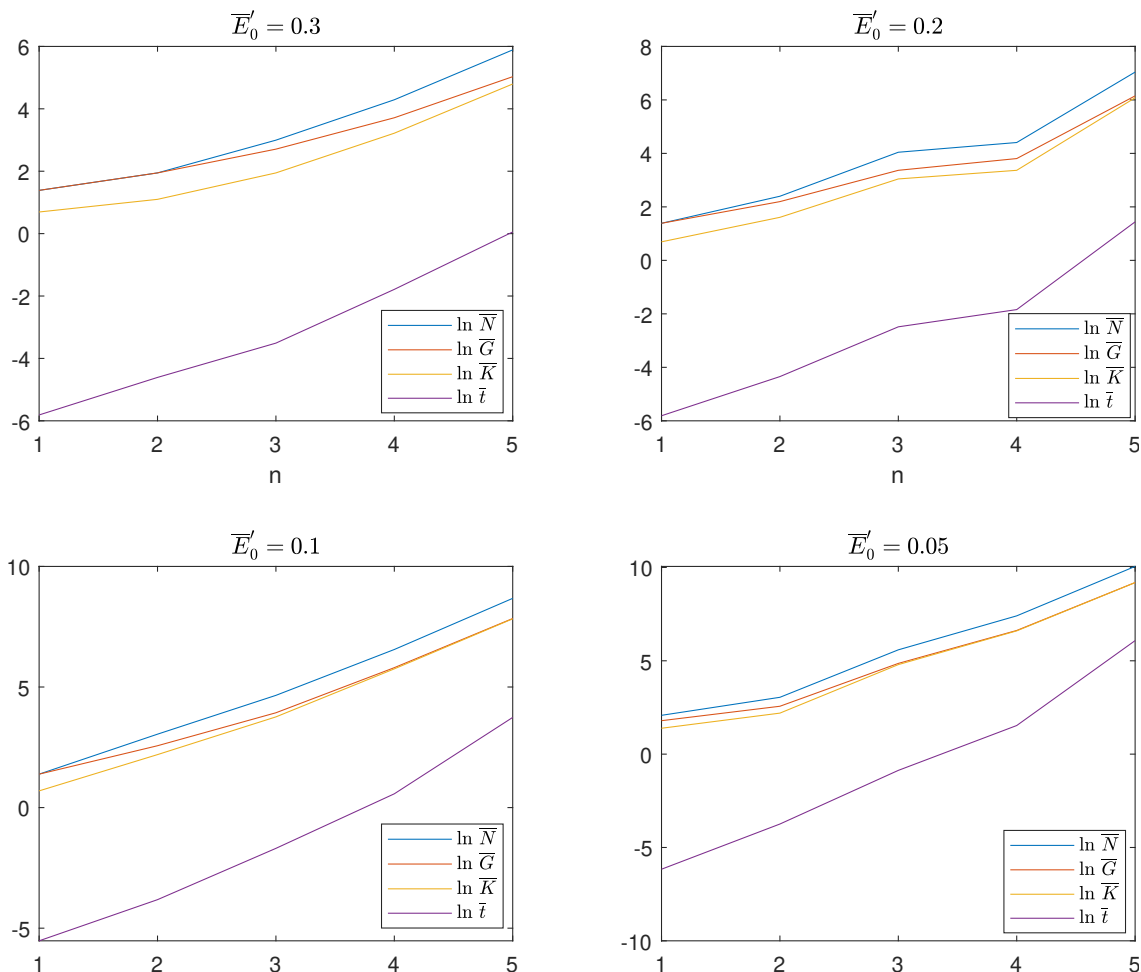


Figure 2: Graphical illustration of the simplicial approximation complexity for quadratic functions.

342 Let us repeat the same tests on hypothetical Cobb-Douglas expected value functions of
 343 the form

$$\mathcal{V}(\mathbf{s}) = \prod_{i=1}^n s_i^{\alpha_i} \quad (\alpha_i \geq 0 \text{ and } \sum_{i=1}^n \alpha_i \leq 1). \quad (22)$$

344 As for the quadratic functions, for each error threshold and each state space dimension, the
 345 simplicial procedure is carried out to construct grid points to approximate the functions,
 346 and five replications are performed. The same statistics are calculated as above. Samples
 347 of results reported in Figure 3 also confirm that the complexity of the simplicial scheme is
 exponential in the state space dimension.

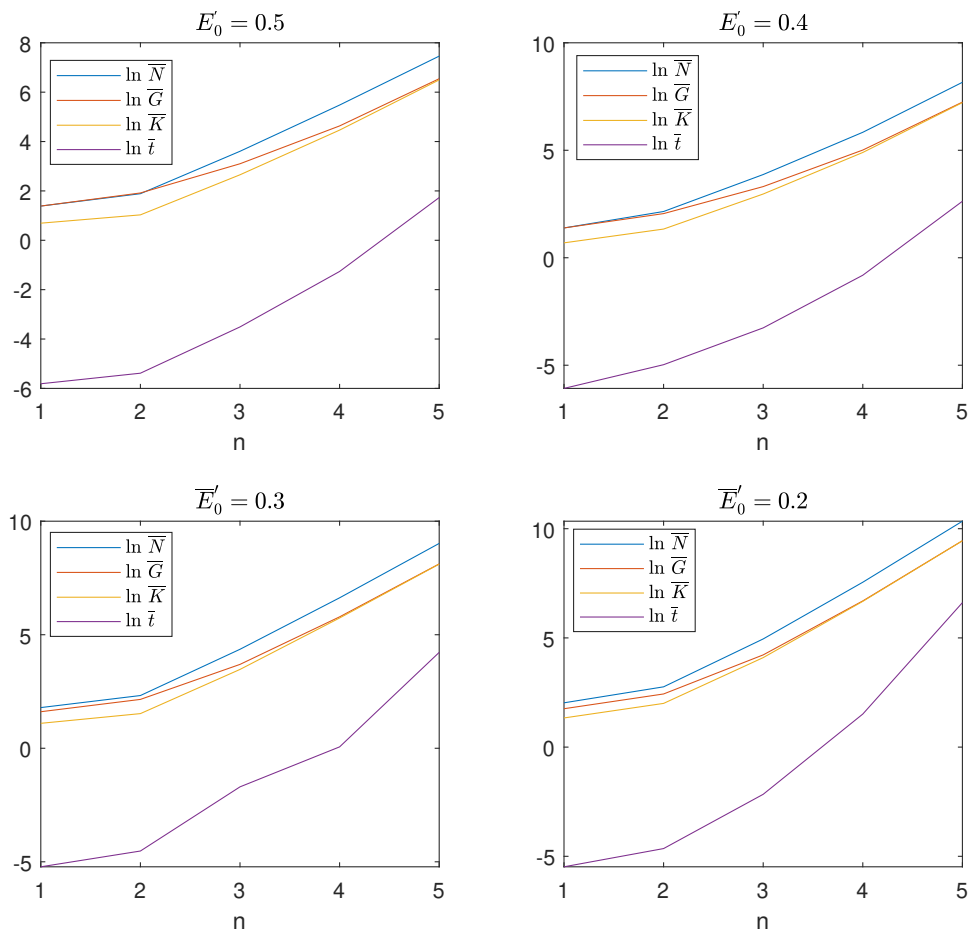


Figure 3: Graphical illustration of the simplicial approximation complexity for concave Cobb-Douglas functions.

348

349 In closing,

350 **Proposition 4.** *The convergence rate of the simplicial algorithm is at best linear.*

351 *Proof.* Since at each iteration the simplex with maximal error bound $\overline{E}_{\mathcal{B}}$ is divided, the
352 simplicial algorithm generates a non-increasing sequence $\{\overline{E}_{\mathcal{B}_k}\}$, such that, by Proposition
353 (3), $\lim_{k \rightarrow \infty} \overline{E}_{\mathcal{B}_k} = 0$. Indeed, at any iteration of the algorithm, assume simplex $\mathcal{B} \subset S$,
354 generated by the matrix $\mathbf{S}_{\mathcal{B}}$, is divided; consider any resulting subsimplex \mathcal{B}^c with generating
355 matrix $\mathbf{S}_{\mathcal{B}^c}$. Matrices $\mathbf{S}_{\mathcal{B}}$ and $\mathbf{S}_{\mathcal{B}^c}$ differ only by one column. The only column of $\mathbf{S}_{\mathcal{B}^c}$ that
356 is not in $\mathbf{S}_{\mathcal{B}}$ is the division point, $\mathbf{s}_{\mathcal{B}}^*$, of the parent simplex \mathcal{B} , and is a convex combination
357 of the columns of $\mathbf{S}_{\mathcal{B}}$.

358 Now, given that the approximate value function (10)-(16) and its expectation are concave,
359 we have $\sum_{k \in \mathcal{B}} \lambda_k^* \hat{\mathcal{V}}(\mathbf{s}^k, \cdot) \leq \hat{\mathcal{V}}(\mathbf{s}_{\mathcal{B}}^*, \cdot)$, where $\boldsymbol{\lambda}^*$ is the optimal $\boldsymbol{\lambda}$ from Problem (20), and
360 the \mathbf{s}^k 's are the vertices of the parent simplex \mathcal{B} , or the columns of matrix $\mathbf{S}_{\mathcal{B}}$. Thus,
361 we always have $\sum_{k \in \mathcal{B}} \lambda_k^* \hat{\mathcal{V}}(\mathbf{s}^k, \cdot) \leq \sum_{j \in \mathcal{B}^c} \lambda_j \hat{\mathcal{V}}(\mathbf{s}^j, \cdot)$ $0 \leq \lambda_j \leq 1$, where the \mathbf{s}^j 's (one of
362 them being the optimal division point $\mathbf{s}_{\mathcal{B}}^*$) are the extreme points of the subsimplex \mathcal{B}^c .
363 Similarly, due to the concavity of the function, $\hat{\mathcal{V}}(\mathbf{s}_{\mathcal{B}}^*, \cdot) \leq \min_{k \in \mathcal{B}} \{f^k + \mathbf{g}^k \top (\mathbf{s}_{\mathcal{B}}^* - \mathbf{s}^k)\}$ (the
364 extrapolation of the function at $\mathbf{s}_{\mathcal{B}}$). It is also clear that $\min_{j \in \mathcal{B}^c} \{f^j + \mathbf{g}^j \top (\mathbf{s}^c - \mathbf{s}^j)\}$, $\mathbf{s}^c \in$
365 $\mathcal{B}^c\} \leq \min_{k \in \mathcal{B}} \{f^k + \mathbf{g}^k \top (\mathbf{s} - \mathbf{s}^k)\}$, $\mathbf{s} \in \mathcal{B}$.

366 Therefore, due to the concavity of the approximate value function, we always have $\overline{E}_{\mathcal{B}^c} \leq$
367 $\overline{E}_{\mathcal{B}}$, where $\overline{E}_{\mathcal{B}^c}$ and $\overline{E}_{\mathcal{B}}$ are the maximal error bound on the function over subsimplex \mathcal{B}^c and
368 parent simplex \mathcal{B} , respectively. As a result, the error sequence $\{\overline{E}_{\mathcal{B}_k}\}$ is non-increasing, and
369 $\lim_{k \rightarrow \infty} \frac{\overline{E}_{\mathcal{B}_{k+1}}}{\overline{E}_{\mathcal{B}_k}} \leq 1$; and the proof is complete. \square

370 Figure (4) illustrates the convergence of the simplicial algorithm on the approximation
371 of value functions for four midterm reservoir problems. We consider a 10-period planning
372 horizon, and the parameters of the problems are generated as described in the numerical
373 experiment section. For each case, we generate five replications. The grid sizes are fixed at
374 $100n + 2^n$. The evolution of the average relative error (ratio of the error at each iteration to
375 that of the first iteration) for the first period is depicted in Figure (4).

376 As stated in the proof of Proposition (4), we see that the sequence of the approximation
377 error is non-increasing. For the four-dimensional problems, at the last iteration, the initial
378 error is reduced to approximately 20%, and around 75% for the six-dimensional problems,
379 suggesting that denser grid sizes are needed to obtain a similar precision as for the four-
380 dimensional problems.

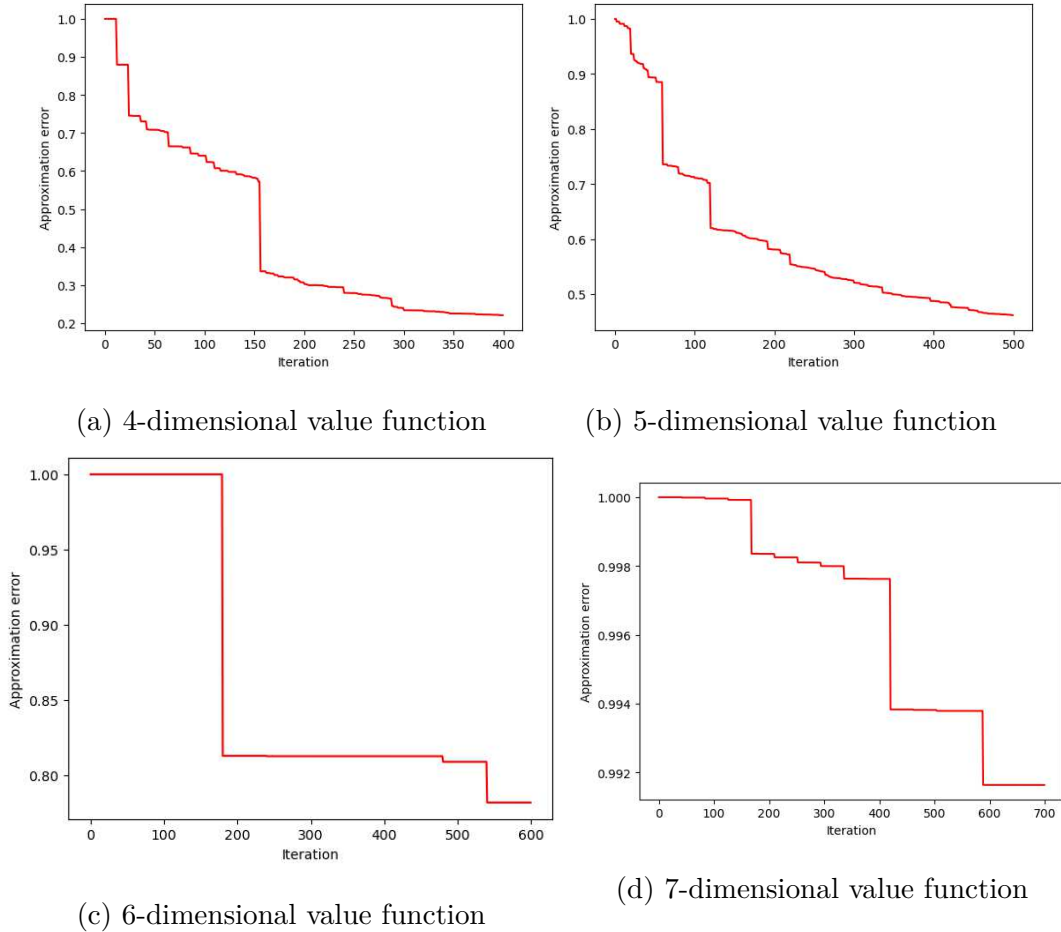


Figure 4: Illustration of the convergence of the simplex algorithm.

381 In general, the approximation error decreases relatively fast over the first few iterations,
 382 then slows down dramatically. This is due to the fact that, as the active simplices (not yet
 383 divided) become smaller, the local curvature of the function does not vary significantly, as a
 384 result, the approximation error is relatively the same on the existing simplices.

385 An apparent disadvantage, especially for state space dimensions greater than or equal
 386 to ten, is the extra computational burden associated with a potentially very large list of
 387 simplices as well as the complete, uniform exploration of the whole state space which may
 388 not be required in practical applications where more localized approximations would be
 389 adequate.

390 Therefore in this paper we seek to explore other ways of constructing grid points to eval-
 391 uate the approximate value function and its expectation in each period without enumerating

392 an exhaustive list of associated simplices in the hope to alleviate the inherent exponential
 393 complexity of the simplicial approach, which is illustrated in the next subsections.

394 4 Hybrid simplicial approximate dynamic programming

395 We now examine some randomized approaches for selecting new grid points at which to
 396 evaluate the approximate value function (10)-(16) in each period t that avoid making a large
 397 list of active simplices. With these approaches, it is not possible to identify a division point
 398 of largest error bound, so there is a need for statistical estimation of the approximation error,
 399 and other heuristics must be called upon for selecting a new grid point at each iteration.
 400 We first describe three such heuristics and next we discuss statistical estimation of the
 401 approximation error.

402 4.1 Randomized simplex-based sampling of the reservoir level space

403 **Monte Carlo (MC).** Instead of using a regular grid of equally spaced vertices, one simple
 404 and very crude approach is to use a sequence of pseudo-random vertices. In each period
 405 t , let \mathbf{v}^k be a sequence of n -vectors of independent variates, uniformly distributed in $[\mathbf{0}, \mathbf{1}]$.
 406 Again, we drop the time period index t for ease of notation. Starting with the initial set of
 407 2^n extreme points of the hyperrectangle S , the i -th component of the k^{th} random vertex is
 408 given by $s_i^{(2^n+k)} = \underline{s}_i + (\bar{s}_i - \underline{s}_i)v_i^k$, for $i = 1, \dots, n$.

409 This naïve random sequence of approximation nodes can be considered neutral with
 410 respect to the approximation error in the sense that the choice of the next vertex to enter
 411 the support set is not based on an error criterion such as the division point of a simplex with
 412 largest error bound in eq. (20). Therefore one would expect that a numerical comparison of
 413 this naïve scheme with the previous method would show a significant difference in accuracy.

414 **MC simplicial.** This method is a combination of the simplicial and the Monte Carlo
 415 schemes. In period t , suppose the approximate value function has been evaluated at K
 416 points. We then generate a random point $\hat{\mathbf{s}}$ uniformly in S as before ($\hat{s}_i = \underline{s}_i + (\bar{s}_i - \underline{s}_i)v_i$),
 417 solve eq. (18) to find the vertex set $\mathcal{B}(\hat{\mathbf{s}})$ of the simplex containing $\hat{\mathbf{s}}$ and solve eq. (20) to
 418 obtain the division point $\mathbf{s}_{\mathcal{B}}^*$ that has the largest error bound in that simplex. Lastly, we

419 choose that division point as the new vertex $\mathbf{s}^{K+1} = \mathbf{s}_{\mathcal{B}}^*$. This procedure is repeated until
 420 the size of the grid reaches a desired target.

421 **Batch MC simplicial.** As in the MC simplicial method, in period t , suppose at a given
 422 iteration there are K vertices in the grid, with $K \geq n + 1$. Next, we generate a sample of m
 423 random points $\hat{\mathbf{s}}^1, \dots, \hat{\mathbf{s}}^m$ uniformly in S . For each random point $\hat{\mathbf{s}}^j$ in the sample, eq. (18)
 424 is solved to find the vertex set \mathcal{B}^j of the simplex that contains $\hat{\mathbf{s}}^j$, and eq. (20) to obtain the
 425 division point $\mathbf{s}_{\mathcal{B}^j}^*$ that has the largest error bound $\bar{E}_{\mathcal{B}^j}$ in that simplex. Then the new vertex
 426 is chosen as the division point of the simplex with the largest error bound in the sample, so
 427 $\mathbf{s}^{K+1} = \mathbf{s}_{\mathcal{B}^{j^*}}^*$ where $j^* = \arg \max_{j=1, \dots, m} \bar{E}_{\mathcal{B}^j}$. This way, by evaluating a small number m of
 428 simplices, we have good chances of choosing a candidate with a relatively large error bound,
 429 but without having to maintain a large list of simplices as in the previous papers.

430 By keeping one candidate out of m at each iteration, the best we can hope for is that
 431 the selected vertices would belong to the top $(1/m)$ th among the sampled candidates. But
 432 there is a probability $(1 - 1/m)^m$ that the selected vertex is not in the top $(1/m)$ th, and also
 433 some probability that the sample has more than one candidate in the top $(1/m)$ th, so that
 434 good candidates are discarded in some iterations. With $m = 3$, these probabilities are $8/27$
 435 (select bad vertex) and $7/27$ (discard good vertex). While this seems better than the MC
 436 and the MC simplicial methods, where all vertices are selected (good and bad), we can try
 437 to improve the selection process by putting some candidate vertices in a waiting line instead
 438 of discarding them right away.

439 **Batch MC simplicial with queue.** As in the batch MC simplicial method, but now,
 440 we keep a list, of at most r recently explored simplices, which have been queued from previous
 441 iterations instead of being discarded. Initially, the queue is empty. In a typical iteration,
 442 m new candidates are sampled as in the batch MC simplicial method, which are combined
 443 into a pool with the (at most) r candidates from the queue. The new vertex is chosen as
 444 the division point of the simplex with the largest error bound in the pooled candidate list.
 445 The next r candidates with largest error bounds are held in the queue, and the remaining
 446 candidates with the smallest error bounds are discarded.

447 Parameters for this would need to be experimented if this turns out to be a tempting
 448 avenue. The computational effort is similar to the batch MC simplicial method but it is

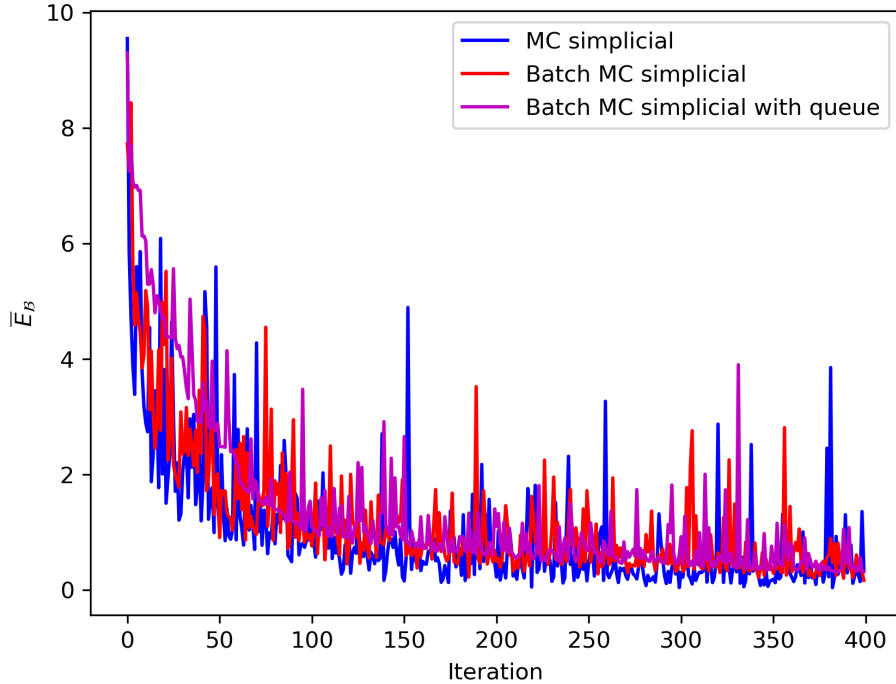


Figure 5: Illustration of the convergence of the hybrid simplicial methods on the approximation of the first period value function for one of the 4-reservoir literature test problems described in Subsection (5.3).

449 hoped that the batch MC simplicial with queue would have smaller approximation error
 450 than the batch MC simplicial.

451 The above methods attempt to replace an exhaustive list of simplices with a shorter
 452 list from which a division point is chosen with the largest error bound at each step. It is
 453 hoped that the use of a truncated candidate list will be compensated by the large number
 454 of sampled points and simplices over a large number of steps. However, in the absence of
 455 an exhaustive list of simplices, there is no uniform upper bound on the approximation error.
 456 Also, as it is illustrated in Figure 5, in contrast to the simplicial scheme, there is no guarantee
 457 about the monotonicity of the sequence of generated approximation errors. Thus, the next
 458 section will discuss the statistical estimation of error.

459 An illustrative comparison between the original and the hybrid simplicial methods is
 460 provided in Appendix B.

461 4.2 Statistical estimation of the approximation error

462 Under the concavity of the expected value function $\hat{\mathcal{V}}_t(\mathbf{s}_t, \cdot)$, the approximation error is the
 463 difference between the function and its piecewise linear approximation. At any point $\mathbf{s}_t \in S_t$,
 464 the approximation error is $\hat{\mathcal{V}}_t(\mathbf{s}_t, \cdot) - B_L(\mathbf{s}_t)$, where $B_L(\mathbf{s}_t)$ solves eq. (18). Then eq. (19)
 465 implies the approximation error is bounded by $B_U(\mathbf{s}_t) - B_L(\mathbf{s}_t)$. At all points in simplex
 466 \mathcal{B} that contains \mathbf{s}_t , the approximation error is bounded by $\bar{E}_{\mathcal{B}}$ of eq. (20), while the largest
 467 error in the simplex is $E_{\mathcal{B}}$ of eq. (21). Here we are interested in the estimation of the largest
 468 actual error $\max_{\mathbf{s}_t \in S_t} \{\hat{\mathcal{V}}_t(\mathbf{s}_t, \cdot) - B_L(\mathbf{s}_t)\}$ or the largest error bound $\max_{\mathcal{B}} \bar{E}_{\mathcal{B}}$. In both cases,
 469 we will use a random sample of m points $\hat{\mathbf{s}}^1, \dots, \hat{\mathbf{s}}^m \in S$.

470 Since function $\hat{\mathcal{V}}_t(\mathbf{s}_t, \cdot)$ is finite and concave everywhere on S_t , by construction, the ap-
 471 proximation error is also a well-behaved function; it is equal to zero at the support nodes
 472 and varies smoothly on the simplices. Therefore, when sampling the state space uniformly,
 473 it might be reasonable to assume that the corresponding distribution of the approximation
 474 error is also well-behaved. However, since we do not know the theoretical distribution, first,
 475 we conduct an empirical investigation. Toward this end, we generate samples of grid points
 476 with the different randomized methods - except for the pure Monte Carlo and the simplicial
 477 methods, and calculate the true approximation errors for random sample points. Examples
 478 of empirical distributions are illustrated in Figure 6. The true empirical distribution seems
 479 to be bounded by a uniform distribution, or a left triangular distribution with mode at the
 minimum value, or a right triangular distribution with mode at the maximum value.

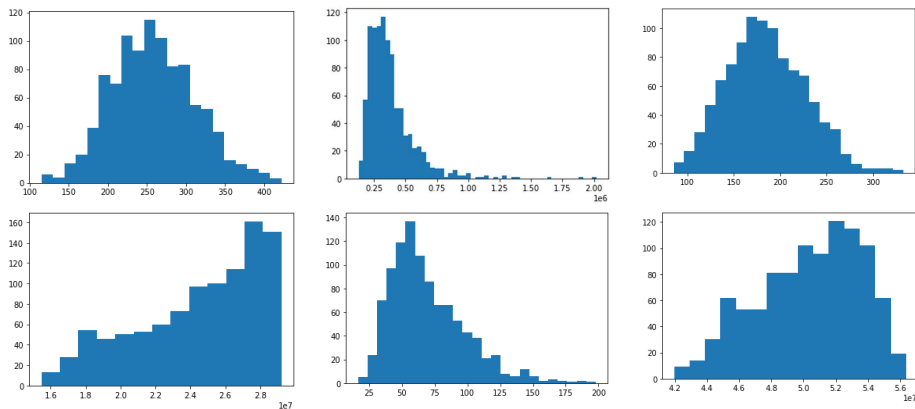


Figure 6: Examples of empirical distributions of the approximation errors.

481 Therefore, we propose to use, as statistical models, three simple distributions on $(0, b)$:
 482 the right-angled triangular with mode at right TR $(0, b)$, the uniform U $(0, b)$, and the right-
 483 angled triangular with mode at left TL $(0, b)$.

484 If a random variable X has a uniform distribution on the interval $[0, b]$, then it is well
 485 known, see e.g. [26], that the maximum likelihood estimator (MLE) of the parameter b is the
 486 largest observation in the sample. So with sample size m and observed values x_1, \dots, x_m ,
 487 the MLE of b is $x_{(m)} = \max_{i=1, \dots, m} x_i$. Estimators of the limit parameters of a right-angled
 488 triangular distribution on the interval $[a, b]$, with the mode at the upper limit b , are given in
 489 [34], where it is shown that the MLE of b is also $x_{(m)}$. However, by arguing as in [36], it is
 490 easily seen that $x_{(m)}$ is not an MLE of b for a right-angled triangular distribution with the
 491 mode at the lower limit. The true MLE is provided in Appendix C.

492 In addition to the point estimates of parameter b , it is useful to obtain confidence intervals.
 493 For this, it is convenient to define the standardized random variable Y with distribution on
 494 the unit interval $[0, 1]$. For a random sample of m observations, we define the largest of them
 495 by $y_{(m)}$, with the random variable $Y_{(m)}$ representing its sampling distribution. Let $F_m(y)$ be
 496 the cumulative distribution function of $Y_{(m)}$. Then $p = F_m(y)$ is the cumulative probability
 497 and $y = F_m^{-1}(p)$, the quantile. Formulas for these are given in Table 1.

	TR $(0, b)$	U $(0, b)$	TL $(0, b)$
$p = F_m(y)$	y^{2m}	y^m	$[1 - (1 - y)^2]^m$
$y = F_m^{-1}(p)$	$p^{1/2m}$	$p^{1/m}$	$1 - \sqrt{1 - p^{1/m}}$

Table 1: Formulas for sampling distributions and quantiles.

498 Formulas for unbiased point estimates, \hat{b} , of parameter b with lower and upper limits of
 499 confidence intervals are given in Table 2 as multipliers of $x_{(m)}$, where

$$A_m = \prod_{j=1}^m \frac{j}{j + 0.5}, \quad (23)$$

500 from adapting equation (6) of [34].

501 A numerical example is given in Table 3. For the triangular distribution with mode at
 502 left TL $(0, b)$, we see that the unbiased estimate and confidence interval limits based on the

	TR(0, b)	U(0, b)	TL(0, b)
$\hat{b}_{1-\alpha/2}$	$\frac{1}{(1-\alpha/2)^{1/2m}}$	$\frac{1}{(1-\alpha/2)^{1/m}}$	$\frac{1}{1-\sqrt{1-(1-\alpha/2)^{1/m}}}$
\hat{b}	$\frac{2m+1}{2m}$	$\frac{m+1}{m}$	$\frac{1}{1-A_m}$
$\hat{b}_{\alpha/2}$	$\frac{1}{(\alpha/2)^{1/2m}}$	$\frac{1}{(\alpha/2)^{1/m}}$	$\frac{1}{1-\sqrt{1-(\alpha/2)^{1/m}}}$

Table 2: Formulas for unbiased point estimate \hat{b} of b and limits of confidence interval.

503 order statistic $x_{(m)}$ are quite large compared to the other distributions. There might be an
504 interest here in using an MLE estimate instead, which has small bias and smaller variance
505 as pointed out in [36] thus allowing a smaller sample size for estimating the approximation
506 error, and therefore fewer computations.

Symbol	TR(0, b)		U(0, b)		TL(0, b)	
m	3	30	3	30	3	30
$\hat{b}_{1-\alpha/2}$	10.04	10.00	10.08	10.01	11.01	10.30
\hat{b}	11.67	10.17	13.33	10.33	18.42	11.90
$\hat{b}_{\alpha/2}$	18.49	10.63	34.20	11.31	62.97	15.16

Table 3: Numerical example for point estimate \hat{b} of b and confidence interval with $m = 3$ and 30, $\alpha = 0.05$ and $x_{(m)} = 10$.

507 5 Numerical experiments

508 Three types of analysis are carried out in the numerical experiments. First, in Subsection 5.1,
509 we appraise the sensitivity of the performance of the two Monte Carlo simplicial methods with
510 respect to their underlying parameters. Second, in Subsection 5.2 the methods are compared
511 on the trade-off between accuracy and computational burden on (i) the approximation of
512 concave functions; and (ii) several simulated reservoir optimizations problems. Lastly, in
513 Subsection 5.3, we compare the methods on three reservoir optimization problems available

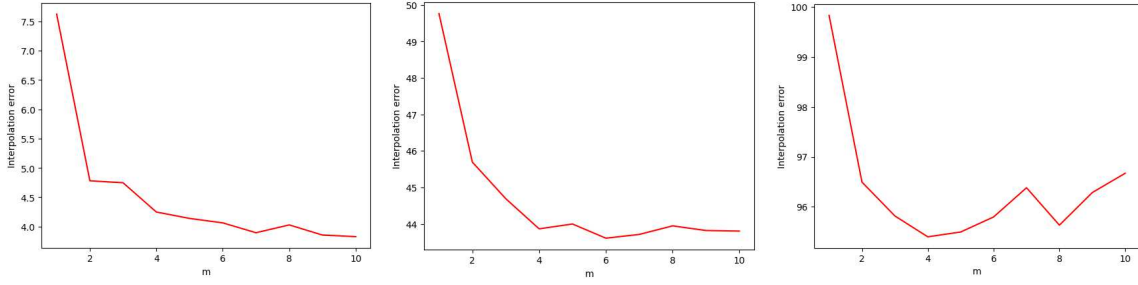
514 in the literature.

515 **5.1 Sensitivity of solution performance to parameter values: batch** 516 **MC simplicial and bath MC simplicial with queue methods**

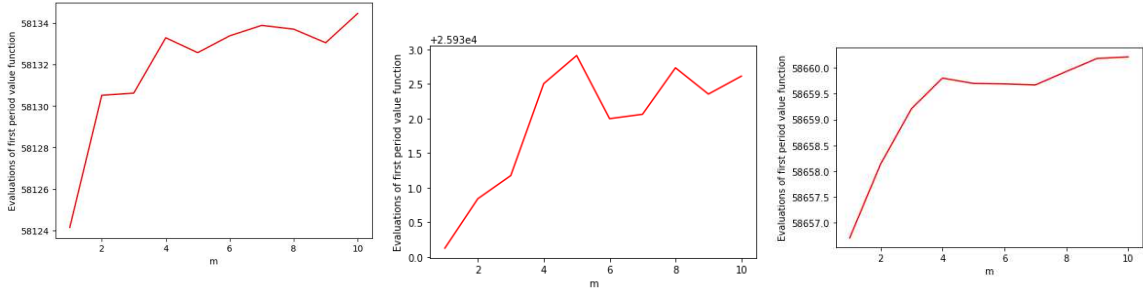
517 Recall that in the batch MC simplicial method, in each period t , at each iteration, a sample of
518 m random points is chosen in the state space, S_t . Intuitively, this approach is approximately
519 m times slower than the MC simplicial scheme, in which one random point is selected at each
520 iteration. One natural question is how to determine the appropriate sample size m . Though
521 we do not have any theoretical answer to this question, we perform numerical experiments to
522 analyze the sensitivity of solution performance on the approximations of Cobb-Douglas type
523 functions (in dimension $n=3, 6$, and 9 , respectively), with randomly generated parameters,
524 and the approximation of value functions for reservoir management problems (in dimension
525 $n=3, 4$, and 6 , respectively).

526 We approximate the Cobb-Douglas functions on grids of size $100n$, then interpolate the
527 values of the functions on other grids (out-of-sample) of size $200n$ (solving Problem (18))
528 and calculate the true approximation errors. For the reservoir management problems, we
529 approximate the value functions (in each time period) on grids of size $100n$ as well, then
530 solve the first period problem for a sample of $200n$ ($\mathbf{s}_1, \mathbf{q}_1$) state pairs. For each case (Cobb-
531 Douglas function approximations and value function approximations), five replications are
532 performed for values of m ranging from one to ten. The average results are reported in
533 Figure 7. Note that smaller values are better in the upper portion of the figure, and the
534 opposite in the lower portion of the figure. The figure displays an “imperfect elbow shape”,
535 and seems that values of m between three to five would suffice to obtain good approximation
536 performance. The computational burden grows linearly with the parameter m ; since we
537 strive for a good trade-off between computational burden and accuracy, in the sequel, we
538 will fix m at 3.

539 Similarly, the batch MC simplicial with queue method features two parameters m (same
540 as the previous method), and r , the size of the queue of previously generated random points.
541 We perform the same experiments as above to assess the sensitivity of solution performance



(a) Interpolation errors of 3-dimensional Cobb-Douglas functions. (b) Interpolation errors of 6-dimensional Cobb-Douglas functions. (c) Interpolation errors of 9-dimensional Cobb-Douglas functions.



(d) First period 3-dimensional value function values. (e) First period 4-dimensional value function values. (f) First period 6-dimensional value function values.

Figure 7: Performance of the batch MC simplicial method on different types of problems and by sample size.

542 with respect to these parameters. We vary the values of m between one and six (based on the
543 above observations), and the values of r between one and eight. Overall, the computational
544 burden is linear in m , and does not seem to be influenced by the length of the queue, r
545 (Figure 8); similarly for the performance of the solution (Figure 9). In addition, in Figure 9,
546 in most of the cases, for fixed value r , we observe an elbow shape at $m = 3$ (except for the last
547 picture), suggesting that $m = 3$ seems to be a good enough sample size. Extensive numerical
548 experiments have demonstrated that this method exhibits similar performance (both in terms
549 of computational burden and accuracy) than the batch MC simplicial scheme; thus, results
550 for this method will not be reported in the sequel for the sake of brevity.

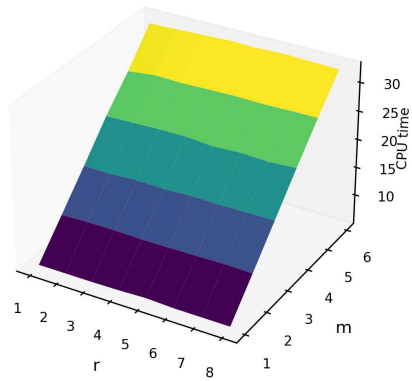
551 **5.2 Accuracy vs computational burden**

552 Here, we focus on the trade-off between accuracy and computation time. Toward this end,
553 first, in Subsection 5.2.1, we compare the performance of the methods on the approximation
554 of Cobb-Douglas concave functions of the form (22) for different state dimensions n . Though
555 the primary interest of this work is mid-term reservoir management problem, this first set-
556 ting is motivated by the fact that (i) the simplex-based approximations exploit the concavity
557 property of the functions to be approximated, in contrast to the pure Monte Carlo (MC)
558 scheme; (ii) in the reservoir management context, to handle the nonlinearity of the produc-
559 tion functions, we approximate the latter by piecewise concave linear functions (Problem
560 (10)-(16)); (iii) similarly, the value functions are approximated by piecewise concave lin-
561 ear functions (Problem (10)-(16)). Thus, it is no easy task isolating the sole effects of the
562 methods, due to the multiple layers of approximation embedded in the dynamic programs.

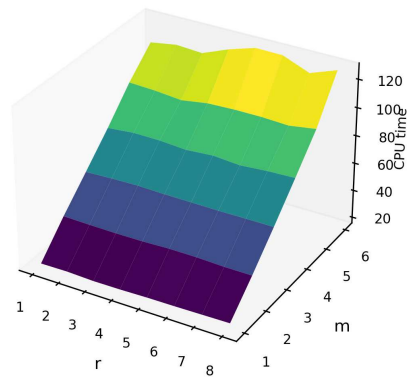
563 Next, in Subsection 5.2.2, the schemes are gauged on several simulated reservoir man-
564 agement problems.

565 **5.2.1 Approximation of concave functions**

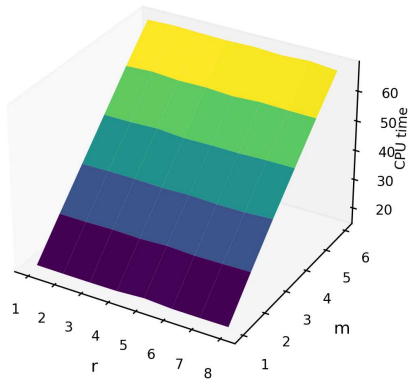
566 Grid points of size $2^n + 100n$ are generated with each method; then the out-of-sample in-
567 terpolation errors - the difference between the true and interpolated values- are calculated
568 on randomly generated samples of sizes $200n$. In addition, under each method and at each



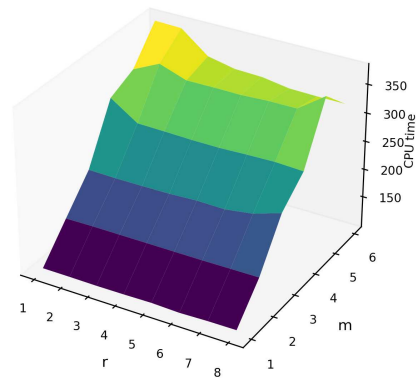
(a) Interpolation of 6-dimensional Cobb-Douglas functions.



(b) Interpolation of 10-dimensional Cobb-Douglas functions.

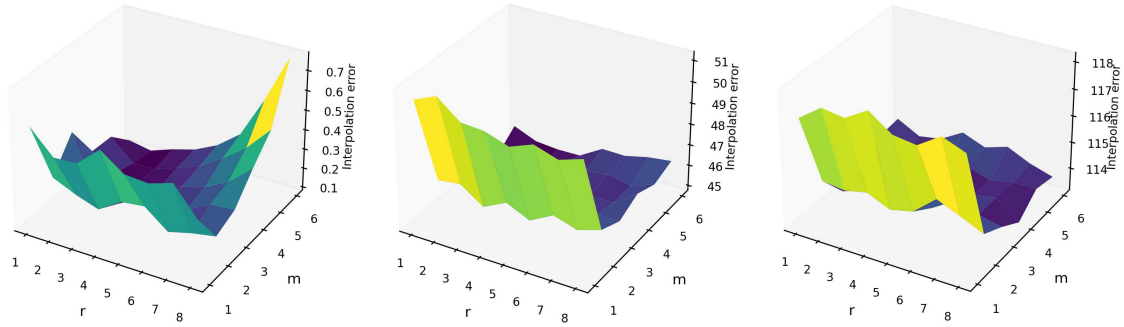


(c) Approximation of 3-dimensional first period value functions.

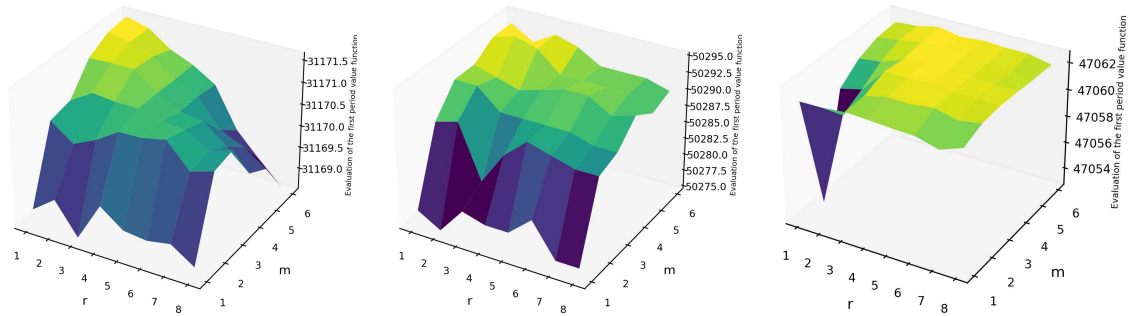


(d) Approximation of 4-dimensional first period value functions.

Figure 8: Average CPU time in seconds of the batch MC simplicial with queue method for different types of problems and by sample size.



(a) Interpolation errors of 2-dimensional Cobb-Douglas functions. (b) Interpolation errors of 6-dimensional Cobb-Douglas functions. (c) Interpolation errors of 10-dimensional Cobb-Douglas functions.



(d) Approximation of 2-dimensional first period value functions. (e) Approximation of 3-dimensional first period value functions. (f) Approximation of 4-dimensional first period value functions.

Figure 9: Performance of the batch MC simplicial with queue method on different types of problems and by sample size.

569 iteration, we record the time in seconds to build the grid (t_i), the minimum (E_{\min}), the max-
570 imum (E_{\max}), the mean (E_{av}), and the standard deviation of the interpolation error (E_{std}).
571 We take the simplicial method as our benchmark, and for each method, we calculate relative
572 performance measures as the ratio of the corresponding measure to that of the simplicial.
573 Furthermore, in addition to the relative computation times (in seconds), we also report
574 the absolute times. The results are depicted in Table 4.

575 As expected, the pure MC method is the fastest as no additional optimization problem
576 is solved except for the approximate dynamic Problems (10)-(16). Also, notice that as
577 we conjectured, the batch MC simplicial scheme is about three times slower than its MC
578 simplicial counterpart, as in the former, in each iteration, we generate three sample points,
579 compared to one in the latter. For 3-dimensional functions, the average CPU time of the
580 simplicial method is lower than that of the MC simplicial scheme; for 5-dimensional problems,
581 the computation times are comparable. For dimensions equal to eight, the relative average
582 CPU time of the MC simplicial method is only 3% that of the simplicial benchmark, which
583 becomes practically intractable for 10-dimensional problems.

584 Accuracy-wise (average interpolation errors), except for the 3-dimensional problems on
585 which it performs better than the pure MC scheme, the simplicial approach features the
586 worst performance. The batch MC simplicial is the top performer on all cases, followed by
587 its MC simplicial counterpart; however, the difference grows smaller as the dimensions of the
588 functions increase, and the MC simplicial scheme still remains about three times faster.

589 Furthermore, we test the scalability of the randomized methods on the approximation of
590 11- to 15-dimensional Cobb-Douglas concave functions. As above, we use all the methods,
591 but the simplicial one (as it is intractable for such high-dimensional problems) to generate
592 sample points of size $2^n + 100n$; then interpolation errors are calculated on samples of
593 size $100n$. We also perform five replications with each method and calculate the same
594 performance statistics, which are reported in Table 5. In addition to being tractable for
595 all the cases, the hybrid methods still outperform the naïve approach (MC) in terms of the
596 maximum and average interpolation errors; they also feature lower standard deviations of the
597 approximation errors. The batch MC simplicial method still outperforms the MC simplicial
598 one, but at the expense of higher computation time.

n	Method	Abs. CPU time	Relative averages				
			\bar{t}_i	\bar{E}_{\min}	\bar{E}_{\max}	\bar{E}_{av}	\bar{E}_{std}
3	Monte Carlo (MC)	0.0053	0.0052	0.5900	16.9683	3.0710	11.0501
3	MC simplicial	2.6148	2.5680	0.5494	6.7624	0.9346	3.3748
3	Batch MC simplicial	7.1774	7.0491	0.7292	1.5631	0.5604	0.9166
3	Simplicial	1.0182	1	1	1	1	1
5	Monte Carlo (MC)	0.0195	0.0032	0.2967	1.9246	0.7857	1.9677
5	MC simplicial	6.8779	1.1196	0.3354	0.9538	0.3653	0.7031
5	Batch MC simplicial	21.8420	3.5556	0.4331	1.0314	0.3080	0.5134
5	Simplicial	6.1430	1	1	1	1	1
8	Monte Carlo (MC)	0.0353	0.0001	0.2867	0.9061	0.5261	1.1074
8	MC simplicial	10.5880	0.0347	0.3358	0.5883	0.3364	0.5819
8	Batch MC simplicial	32.6510	0.1070	0.3689	0.5450	0.3217	0.4596
8	Simplicial	305.2224	1	1	1	1	1
10	Monte Carlo (MC)	0.0891	0.0000	0.3499	0.9094	0.6171	1.2257
10	MC simplicial	22.1880	0.0003	0.4115	0.7349	0.4438	0.7686
10	Batch MC simplicial	66.3756	0.0010	0.5561	0.6184	0.4227	0.5881
10	Simplicial	64,544.1457	1	1	1	1	1

Table 4: Statistics pertaining to interpolation errors of Cobb-Douglas concave functions.

5.2.2 Simulated mid-term reservoir optimization problems

As in [63], for each plant $i = 1, \dots, n$, we assume the production function to be of the form

$$p_{it}(u_{it}) := \beta_i ((u_{it} + \gamma_i)^{\alpha_i} - \gamma_i^{\alpha_i}), \quad \beta_i > 0, \quad \gamma_i \geq 0, \quad 0 \leq \alpha_i \leq 1 \quad (24)$$

These production functions are linearized as in (10)-(16). Furthermore, we consider a planning horizon of length $T=10$, and three reservoir configurations in dimension $n = 4, 6, 8$, respectively. The problems' parameters, including bounds on the reservoir and water release levels, borrowed from [65], are shown in Table 6.

For each reservoir configuration, problem instances are randomly generated based on the

n	Method	\bar{t}_i	\bar{E}_{\min}	\bar{E}_{\max}	\bar{E}_{av}	\bar{E}_{std}
11	MC	0.344	59.028	412.691	218.829	59.242
11	MC simplicial	58.226	81.156	326.580	181.372	40.439
11	Batch MC simplicial	172.198	89.063	324.405	178.096	34.672
12	MC	0.654	68.220	355.558	199.278	47.175
12	MC simplicial	104.374	81.156	300.623	171.980	32.605
12	Batch MC simplicial	308.748	97.082	285.989	169.595	28.850
13	MC	1.420	82.863	380.341	226.818	48.482
13	MC simplicial	191.568	108.638	329.196	199.129	34.918
13	Batch MC simplicial	583.787	107.968	317.029	197.336	31.458
14	MC	2.649	92.604	392.457	234.484	45.704
14	MC simplicial	350.843	117.821	339.119	209.566	33.505
14	Batch MC simplicial	1,035.349	119.204	323.903	208.207	30.196
15	MC	5.803	101.726	348.771	220.790	37.342
15	MC simplicial	717.993	110.628	312.374	204.199	27.734
15	Batch MC simplicial	2,265.467	127.493	301.875	203.217	26.217

Table 5: Statistics pertaining to interpolation errors of 11- to 15-dimensional Cobb-Douglas concave functions using the hybrid methods.

606 experimental framework depicted in Table 6. To mitigate boundary effects, the terminal
607 value function, $\mathcal{V}_{T+1}(s_{T+1})$, is chosen as a concave function of the form (22).

608 In addition, in each period of the planning horizon, we use each method to generate
609 samples of $2^n + 200n$ grid points to evaluate the approximate value function (10)-(16). Then,
610 we randomly generate a sample of $1,000n$ initial reservoir levels and natural inflows. Next,
611 as in [12], the first period approximate problem is solved with each method for each state
612 observation of the sample, and we record the minimum ($V_{1\min}$), the maximum ($V_{1\max}$), the
613 average ($V_{1\text{av}}$), and the standard deviation ($V_{1\text{std}}$) of the first period value function evaluation.
614 Five replications are performed for each case, then we calculate the average of each such
615 statistic as well as the average time (\bar{t}_i) to build the 10 value functions. As in the above

Parameter	Lower limit	Upper limit
\underline{s}_{it}	150	600
\bar{s}_{it}	800	7,000
\underline{u}_{it}	0	0
\bar{u}_{it}	$0.05\bar{s}_{it}$	$1.5\bar{s}_{it}$
β_i	0.9	1.5
α_i	0.7	0.9
γ_i	$125u_i$	$170u_i$
q_{it}	500	3,000

Table 6: Model parameters borrowed from [65].

616 comparisons, we take the simplicial scheme as the benchmark method. The results (relative
617 measures) are reported in Table 7 as well as the average absolute CPU times (in seconds).

618 Again, without any surprise, the pure MC method is the fastest. The average CPU time
619 is relatively the same under the simplicial and its MC simplicial variant on the 4-dimensional
620 problems; the latter scheme features lower computational burden on the 6- and 8-dimensional
621 instances. Both hybrid methods outperform the simplicial scheme on all the other metrics on
622 the 6-dimensional problems. The performance of the methods is similar on the 8-dimensional
623 problems, however at lower computational burden for the MC variant methods. Indeed, the
624 CPU time of the MC method is approximately 2% of that of the simplicial scheme, and 4%
625 and 9%, for the MC simplicial and its batch variant, respectively.

626 We close this section with an analysis of the sensitivity of the solution accuracy of the
627 different methods to the size of the grids. We repeat the above experiments on 4- and
628 6-dimensional reservoir problems. The parameters are generated as in Table 6.

629 In each period, for each problem, we construct grids of sizes varying between $K_1 =$
630 $2^n + 20n$, and $K_5 = 2^n + 100n$, in increment of $20n$. As before, the first period value
631 functions are solved for $1,000n$ randomly generated initial reservoir levels and inflows, then
632 the average is taken. For each grid size $K_j, j = 2, \dots, 5$, Table 8 depicts the relative average
633 value function $\frac{\bar{V}_j}{\bar{V}_{j-1}}$. The results show that the average evaluations of the first period value

n	Method	$\overline{\text{Abs. CPU time}}$	Relative averages				
			\bar{t}_i	$\overline{V}_{1\min}$	$\overline{V}_{1\max}$	$\overline{V}_{1\text{av}}$	$\overline{V}_{1\text{std}}$
4	Monte Carlo (MC)	10.0974	0.2921	1.0001	1.0006	1.0006	0.9996
4	MC simplicial	30.7411	0.8892	1.0012	1.0012	1.0012	0.9979
4	Batch MC simplicial	76.9120	2.2248	1.0012	1.0012	1.0012	0.9977
4	Simplicial	34.5699	1	1	1	1	1
6	MC	105.5044	0.3082	0.9954	1.0021	1.0021	1.0131
6	MC simplicial	228.4980	0.6676	1.0026	1.0023	1.0026	1.0030
6	Batch MC simplicial	475.4854	1.3892	1.0029	1.0023	1.0026	1.0020
6	Simplicial	342.2702	1	1	1	1	1
8	MC	158.9624	0.0161	0.9949	0.9952	0.9951	1.0000
8	MC simplicial	433.8685	0.0439	1.0000	1.0000	1.0000	1.0000
8	Batch MC simplicial	882.3298	0.0893	1.0000	1.0000	1.0000	1.0000
8	Simplicial	9,879.5983	1	1	1	1	1

Table 7: Statistics pertaining to the first period evaluations of the value functions for three reservoir configurations ($n = 4, 6, 8$).

634 functions are relatively steady.

635 5.3 Performance comparisons on three literature reservoir man- 636 agement problems

637 Our last comparison setting is three literature reservoir optimization problems: two 4-
638 dimensional and one 10-dimensional problems. The planning horizons are one year divided
639 into monthly time steps. These problems were designed to assess the effectiveness of reservoir
640 optimization solution methods. For details about their characteristics, please see [18, 42, 38].
641 The main difference between the two 4-dimensional problems is that in one of them (hereafter
642 Problem 1), the release decisions are less constrained, and the upper bounds on the reservoirs
643 are stationary (do not vary with time), in contrast with the second one (Problem 2).

644 In all three problems, the first period reservoir level (\mathbf{s}_1) is fixed, similarly for the terminal

n	Method	Grid size				
		$2^n + 20n$	$2^n + 40n$	$2^n + 60n$	$2^n + 80n$	$2^n + 100n$
4	MC	—	1.00017	1.00007	1.00020	1.00022
4	MC simplicial	—	1.00012	1.00003	0.99999	1.00002
4	Batch MC simplicial	—	1.00008	1.00002	1.00001	1.00004
4	Simplicial	—	1.00009	1.00005	1.00006	1.00004
6	MC	—	1.00001	1.00001	1.00000	1.00000
6	MC simplicial	—	1.00002	1.00000	1.00000	1.00000
6	Batch MC simplicial	—	1.00002	1.00000	1.00000	1.00000
6	Simplicial	—	1.00007	1.00023	0.99999	1.00002

Table 8: Variation rate of the average first period value functions with the size of the grid for two reservoir configurations ($n = 4, 6$).

645 one (\mathbf{s}_{13}). Though these constraints can easily be handled in a multi-period model, this is
646 not the case in dynamic programming-like methods, as in period $t = 12$, the algorithms
647 can pick a reservoir level that violates the terminal value constraints on the reservoir levels.
648 Similarly, in any period t , the bounds may also be violated. We mitigate this issue by
649 introducing linearized penalty functions in the objective functions. We calibrate the penalty
650 coefficients through trial-and-errors, until we obtain solutions that meet all the constraints
651 (solving the value functions forward in time as explained below).

652 We build the value functions moving backward in time. Then, starting from the initial
653 reservoir level, we solve the value functions forward in time, using the previous period subop-
654 timal reservoir level as initial value. In each time period, we calculate the suboptimal current
655 period objective value (say the current period suboptimal production in our context). Thus,
656 the suboptimal value of the problem is the sum of such suboptimal objective values.

657 Under each method, we use different grid sizes to build the value functions, as illustrated
658 in Tables 9-14. Under the simplicial method, each problem is solved once (one backward
659 and one forward steps), as the problems are deterministic and the simplicial method is also
660 a deterministic algorithm. Under the hybrid methods, we perform five replications, and

661 calculate the averages (solution times and suboptimal values).

662 Tables 9, 11, and 13 report the optimality gaps (difference between the known optimal
 663 values and the suboptimal ones obtained with the methods) for each grid size and each
 664 method. No results are reported for the simplicial method for the largest problem (10-
 665 dimensional), which proved intractable for this method (we stopped the algorithm after
 666 several hours spent in the last period recursion).

667 The optimality gaps decreases as the grid size increases, regardless of the method. Over-
 668 all, the batch MC simplicial scheme consistently exhibits the lowest optimality gaps, followed
 669 by the MC simplicial method, though the latter is outperformed by the simplicial approach
 670 on the two 4-dimensional problems for the two largest grid sizes. The pure MC method
 671 consistently features the highest optimality gaps. The associated CPU times (in seconds)
 are reported in Tables 10, 12, 14, respectively.

Method	Grid size					
	$2^n + 50n$	$2^n + 100n$	$2^n + 200n$	$2^n + 300n$	$2^n + 500n$	$2^n + 1000n$
MC	1.34%	0.88%	0.67%	0.56%	0.46%	0.40%
Simplicial MC	0.73%	0.49%	0.38%	0.27%	0.26%	0.18%
Batch simplicial MC	0.52%	0.31%	0.19%	0.19%	0.15%	0.11%
Simplicial	1.24%	0.55%	0.53%	0.36%	0.20%	0.15%

Table 9: Optimality gap of the first four-reservoir problem (Problem 1) described in [18, 42] across the tested methods for different grid size.

672

673 6 Conclusions

674 This work has revisited a simplicial approximate stochastic dynamic programming scheme
 675 presented in [63, 64, 65] for the mid-term sub-optimal operations of multi-period multi-
 676 reservoir systems. This iterative method relies on the exhaustive examination of a list of
 677 created simplices, whose vertices define grid points at which the value functions are evalu-

Method	Grid size					
	$2^n + 50n$	$2^n + 100n$	$2^n + 200n$	$2^n + 300n$	$2^n + 500n$	$2^n + 1000n$
MC	0.6255	1.4599	4.2737	8.7034	21.3315	97.0282
Simplicial MC	32.6700	51.0181	196.8790	293.7830	487.9010	1,411.0400
Batch simplicial MC	52.9183	102.4470	225.4920	369.6240	1324.6700	3,024.9700
Simplicial	7.8186	17.4825	64.3685	156.5440	338.2210	1,082.5300

Table 10: CPU time in seconds to approximate the value functions for the first four-reservoir problem (Problem 1) reported in [18, 42] for different grid size across the tested methods.

Method	Grid size					
	$2^n + 50n$	$2^n + 100n$	$2^n + 200n$	$2^n + 300n$	$2^n + 500n$	$2^n + 1000n$
MC	2.86%	2.16%	1.81%	1.75%	1.35%	1.09%
MC simplicial	1.55%	1.21%	0.80%	0.69%	0.52%	0.33%
Batch MC simplicial	1.04%	0.61%	0.40%	0.28%	0.25%	0.19%
Simplicial	1.97%	1.73%	0.89%	0.84%	0.48%	0.28%

Table 11: Optimality gap of the second four-reservoir problem (Problem 2) described in [18, 42, 38] across the tested methods for different grid size.

678 ated at each period. The scheme is limited by the computational burden of partitioning a
679 hypercube into simplices.

680 We have proposed two hybrid methods that combine random sampling strategies with
681 the approach proposed in [63, 64, 65] to locally estimate the approximation error. Simula-
682 tion results of randomly generated and three literature mid-term reservoir management test
683 problems showed that, compared to the simplicial methods, the hybrid methods seem to
684 offer a good trade-off between solution time and accuracy, in particular when the state space
685 dimension is greater than nine. Approximation of functions of dimension up to 15 within
686 reasonable computation time illustrated the potential scalability of the proposed randomized

Method	Grid size					
	$2^n + 50n$	$2^n + 100n$	$2^n + 200n$	$2^n + 300n$	$2^n + 500n$	$2^n + 1000n$
MC	0.6298	1.3913	3.8732	7.7293	18.9845	137.1070
MC simplicial	16.7826	35.4257	87.7464	136.9160	274.4680	1,118.660
Batch MC simplicial	48.6417	102.1330	225.0250	370.3550	725.1740	2,259.890
Simplicial	7.9736	17.7167	81.9990	110.7210	165.5750	954.704

Table 12: CPU time in seconds to approximate the value functions for the second four-reservoir problem (Problem 2) reported in [18, 42, 38] for different grid size across the tested methods.

Method	Grid size					
	$2^n + 50n$	$2^n + 100n$	$2^n + 200n$	$2^n + 300n$	$2^n + 500n$	$2^n + 1000n$
MC	3.15%	3.07%	3.00%	2.73%	2.39%	2.39%
MC simplicial	3.99%	3.21%	2.45%	2.14%	2.20%	1.61%
Batch MC simplicial	4.24%	3.31%	2.73%	2.59%	1.79%	1.31%
Simplicial	n/a	n/a	n/a	n/a	n/a	n/a

Table 13: Optimality gap of the ten-reservoir problem described in [18, 42, 38] across the tested methods for different grid size.

687 methods, which might further be leveraged through parallelization.

688 Appendices

689 A Proof of proposition

690 *Proof of Proposition 2.* We will derive our complexity results in two steps. First, we will
691 show that the error bound on a simplex \mathcal{B} can be approximated by a quadratic function of

704 each off-diagonal position. Furthermore, assuming that at optimality all the inequalities of
 705 (26) are binding, with the only risk of underestimating the error bound, we have the solution:

$$\begin{pmatrix} \boldsymbol{\lambda}_{\mathcal{B}} \\ \phi \end{pmatrix} = \begin{bmatrix} \mathbf{A} & \mathbf{e} \\ \mathbf{e}^\top & 0 \end{bmatrix}^{-1} \begin{pmatrix} \mathbf{f}_{\mathcal{B}} - \mathbf{h} \\ 1 \end{pmatrix}, \quad (27)$$

706 where $\mathbf{A} := -\mathbf{G}_{\mathcal{B}}\mathbf{S}_{\mathcal{B}}$, and $\mathbf{h} := \mathbf{d}\mathbf{S}_{\mathcal{B}}^\top$.

707 It is easy to see that $\begin{bmatrix} \mathbf{A} & \mathbf{e} \\ \mathbf{e}^\top & 0 \end{bmatrix}^{-1} = \begin{bmatrix} \mathbf{A}^{-1} - c\mathbf{A}^{-1}\mathbf{e}\mathbf{e}^\top\mathbf{A}^{-1} & c\mathbf{A}^{-1}\mathbf{e} \\ c\mathbf{e}^\top\mathbf{A}^{-1} & -c \end{bmatrix}$, where the constant $c :=$
 708 $\mathbf{e}^\top\mathbf{A}^{-1}\mathbf{e}$. We then have:

$$\bar{E}'_{\mathcal{B}} := \phi - \mathbf{f}_{\mathcal{B}}^\top \boldsymbol{\lambda}_{\mathcal{B}} = \begin{pmatrix} -\mathbf{f}_{\mathcal{B}} \\ 1 \end{pmatrix}^\top \begin{bmatrix} \mathbf{A}^{-1} - c\mathbf{A}^{-1}\mathbf{e}\mathbf{e}^\top\mathbf{A}^{-1} & c\mathbf{A}^{-1}\mathbf{e} \\ c\mathbf{e}^\top\mathbf{A}^{-1} & -c \end{bmatrix} \begin{pmatrix} \mathbf{f}_{\mathcal{B}} - \mathbf{h} \\ 1 \end{pmatrix}. \quad (28)$$

709 In (28), let $\mathbf{B} := \mathbf{A}^{-1} - c\mathbf{A}^{-1}\mathbf{e}\mathbf{e}^\top\mathbf{A}^{-1}$, an $(n+1) \times (n+1)$ matrix, $\mathbf{b} := c\mathbf{A}^{-1}\mathbf{e}$, an
 710 $n+1$ -dimensional column vector, and $\boldsymbol{\beta}^\top := c\mathbf{e}^\top\mathbf{A}^{-1}$, an $n+1$ -dimensional row vector.
 711 With some algebra, it follows from (28) that:

$$\bar{E}'_{\mathcal{B}} := -\mathbf{f}_{\mathcal{B}}^\top \mathbf{B} \mathbf{f}_{\mathcal{B}} + ((\mathbf{B}\mathbf{h})^\top + \boldsymbol{\beta} + \mathbf{b}^\top) \mathbf{f}_{\mathcal{B}} - \boldsymbol{\beta} \mathbf{h} - c. \quad (29)$$

712 Thus, we see in (29) that the error on simplex \mathcal{B} is a quadratic function of $\mathbf{f}_{\mathcal{B}} \in \mathbb{R}^{n+1}$.

713 Now, we need to find the number of required simplices to guarantee that $\bar{E}'_{\mathcal{B}} \leq \bar{E}_0$.
 714 Though this answer is not straightforward, we argue that this number may depend upon
 715 the dimension n of the state space and the size of the generated simplices. Let $\mathcal{B}(1)$ be a
 716 unit-volume simplex in \mathbb{R}^n , and denote $\mathbf{S}_{\mathcal{B}}(1)$ the matrix formed by its vertices. In addition,
 717 assume this simplex may be scaled by a factor κ to a higher volume simplex $\mathcal{B}(\kappa)$, i.e.,
 718 $\mathcal{B}(\kappa) \sim \kappa\mathcal{B}(1)$.

719 Similarly, assume the matrix of the vertices of $\mathcal{B}(1)$ may be scaled by the same factor κ
 720 to the matrix of $\mathcal{B}(\kappa)$, i.e., $\mathbf{S}_{\mathcal{B}}(\kappa) \sim \kappa\mathbf{S}_{\mathcal{B}}(1)$. Therefore, we can take as an estimate of the
 721 required number of simplices, $N_n(\bar{E}_0)$, the ratio of the volume of the hyperrectangle S to the
 722 volume of a simplex $\mathcal{B}(\kappa)$, such that the error on that simplex does not exceed the desired
 723 threshold, i.e.,

$$N_n(\bar{E}_0) =: \max_{\kappa} \left\{ \frac{\text{Vol}(S)}{\text{Vol}(\mathcal{B}(\kappa))} \mid \bar{E}'_{\mathcal{B}(\kappa)} \leq \bar{E}_0 \right\}. \quad (30)$$

724 Lastly, ignoring the lower order terms in (29), we see that the error bound is a quadratic
 725 function of κ , such that $\overline{E}'_{\mathcal{B}}(\kappa) \sim k_1 \kappa^2$, where k_1 is a proportionality constant. As a result,
 726 to guarantee the desired error threshold \overline{E}_0 , we must have $k_1 \kappa^2 \leq \overline{E}_0$, or

$$\kappa \leq \sqrt{\frac{\overline{E}_0}{k_1}}. \quad (31)$$

727 The volume of a simplex $\mathcal{B}(\kappa)$ being $\text{Vol}(\mathcal{B}(\kappa)) = \frac{1}{n!} \left| \begin{array}{c} \kappa \mathbf{S}_{\mathcal{B}}(1) \\ \mathbf{e}^\top \end{array} \right| = \frac{\kappa^n}{n!} \left| \begin{array}{c} \mathbf{S}_{\mathcal{B}}(1) \\ \mathbf{e}^\top \end{array} \right| := k_2 \frac{\kappa^n}{n!}$, it
 728 follows from the inequality (31) that to guarantee the prescribed error bound, \overline{E}_0 , the volume
 729 $\text{Vol}(\mathcal{B}(\kappa))$ should be of the order $\frac{k_2}{n!} \left(\frac{\overline{E}_0}{k_1}\right)^{n/2}$. Thus, the total number of such simplices should
 730 be:

$$N_{\mathcal{B}} := \frac{\text{Vol}(S)}{\text{Vol}(\mathcal{B}(\kappa))} = \text{Vol}(S) \frac{n!}{k_2} \left(\frac{k_1}{\overline{E}_0}\right)^{n/2}, \quad (32)$$

731 which is of the order $\mathcal{O}\left(\frac{\text{Vol}(S)n!}{(n+1)\overline{E}_0^{n/2}}\right)$. □

732 **B Comparison of the original and hybrid simplicial** 733 **methods**

734 To summarize, we make a brief comparison between the original and hybrid simplicial meth-
 735 ods. Conceptually, the original simplicial method makes an initial list of simplices using
 736 the extreme points of the state set as vertices, for instance via Kuhn's triangulation. The
 737 function to be approximated is evaluated at the vertices, and corresponding subgradients
 738 are calculated. For each simplex in the list, an error bound is obtained by solving eq. (20)
 739 which also returns a division point. Then new vertices are iteratively added by selecting
 740 the simplex with largest error bound in the current list, adding its division point as a new
 741 vertex where the function and subgradient are evaluated, deleting the simplex from the list,
 742 replacing it with the new simplices obtained following its division, and evaluating the error
 743 bounds and division points of the new simplices, and so on. Once a sufficiently large list of
 744 simplices has been obtained, it provides a partition of the state set S . The value function,
 745 call it $f(\mathbf{s})$ for simplicity, at any given point $\mathbf{s} \in S$ is approximated by finding a simplex in
 746 the list containing the point \mathbf{s} and interpolating the (known) function values at its vertices.

747 By contrast, the hybrid methods iteratively build a list of vertices but do not make an
 748 explicit list of simplices. This way, the value function $f(\mathbf{s})$ is approximated at any point
 749 $\mathbf{s} \in S$ by solving the linear program (18) whose optimal basis identifies a set of vertices
 750 that define a simplex containing the point \mathbf{s} . Since the linear program selects the largest
 751 interpolated value among all feasible simplices (not necessary full-dimensional) containing
 752 the point \mathbf{s} , it may provide a better approximation of $f(\mathbf{s})$ than the original simplicial
 753 method in which there is only one full-dimensional simplex containing the point \mathbf{s} . The list
 754 of vertices is obtained iteratively by sampling a point $\hat{\mathbf{s}}$ at random in the state set S , using
 755 eq. (18) to identify an optimal simplex containing the point $\hat{\mathbf{s}}$, then using eq. (20) to find an
 756 error bound and a division point for this simplex, and adding this division point as a new
 757 vertex in the list, and so on.

758 In the original simplicial method, by construction the largest error bound in the list of
 759 simplices provides an upper bound on the approximation error for all points $\mathbf{s} \in S$ although
 760 it might be somewhat overestimated. In the hybrid methods, the error bounds are tighter,
 761 since, as aforementioned, the largest interpolated value is taken among all feasible simplices.

762 To illustrate these ideas, Let us consider the 2-dimensional concave quadratic function:

$$f(s_1, s_2) = 9s_1 + 15s_2 - 2s_1^2 - 5s_1s_2 - (9/2)s_2^2.$$

763 The state set S is the unit square whose vertices are given counterclockwise in Table 15 with
 764 their coordinates and function values:

Vertices	A	B	C	D	Sample \hat{x}
s_1	0	1	1	0	0.6
s_2	0	0	1	1	0.9
$f(s_1, s_2)$	0	7	12.5	10.5	11.835

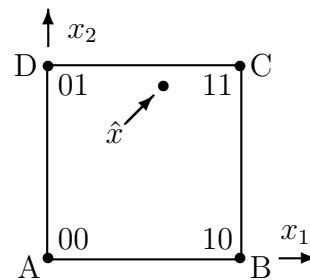


Table 15: Data for quadratic example in two dimensions.

765 Suppose a Kuhn triangulation was used to partition S into the two simplices $ABC := \triangle$
 766 and $ACD := \nabla$. Then eq. (20) would yield an error bound of 3.6964 in both cases with
 767 a division point at $s_1 = s_2 = 0.6786$ for ABC and at $s_1 = s_2 = 0.3214$ for ACD . So the

768 original simplicial method would divide one of the two simplices ABC or ACD at its division
 769 point.

770 By comparison, the MC simplicial method would first sample a point $\hat{\mathbf{s}} \in S$ at random
 771 and then would use eq. (18) to find a simplex over which the interpolation of the function is
 772 the largest at that point $\hat{\mathbf{s}}$. Unlike the original method in which only the simplices already
 773 in the list would be considered, in the MC simplicial scheme all possible simplices would be
 774 taken into account. For example, suppose the coordinates of the sampled point $\hat{\mathbf{s}}$ happened
 775 to be $\hat{s}_1 = 0.6$ and $\hat{s}_2 = 0.9$, the supporting simplex found by eq. (18) would be $BCD := \nabla$
 776 with an interpolated value of 11.15. Next, eq. (20) applied to simplex BCD would find an
 777 error bound of 1.8 with a division point at coordinates $s_1 = 1$ and $s_2 = 0.6$.

778 We notice that if the sampled point $\hat{\mathbf{s}}$ had been interpolated with simplex ACD from the
 779 list, instead of BCD , its interpolated value would have been smaller, i.e., 10.65 instead of
 780 11.15.

781 C MLE estimation of the upper limit of $TL(0,b)$

782 Adapting the approach of [36], it is possible to find a MLE for parameter b by solving a
 783 nonlinear equation. If a random variable X has a right-angle triangular distribution on the
 784 interval $[0, b]$ with mode at the origin, then its density function is

$$g(x) = \begin{cases} \frac{2(b-x)}{b^2} & \text{if } 0 \leq x \leq b, \\ 0 & \text{else,} \end{cases}$$

785 so the likelihood function for an observed sample x is

$$L(x|b) = \frac{2^m \prod_{i=1}^m (b - x_i)}{b^{2m}}$$

786 Then with $\ln L(x|b)$ the first-order optimality condition for the MLE of parameter b is the
 787 nonlinear equation

$$\sum_{i=1}^m \frac{1}{b - x_i} - \frac{2m}{b} = 0, \tag{33}$$

788 which needs to be solved numerically, except in special cases.

789 **Proposition 5.** Let b^* be the unique solution of eq. (33) and let $x_{(m)} = \max_{i=1,\dots,m} x_i$. Then

$$\frac{m+1}{m} \times x_{(m)} \leq b^* \leq 2x_{(m)}. \quad (34)$$

790 *Proof.* When $x_{(m)} > 0$, the bounds in eq. (34) are attained in the extreme cases with $x_1 =$
 791 $\dots = x_{m-1} = 0$ for the lower bound, and $x_1 = \dots = x_m = x_{(m)}$ for the upper bound. In the
 792 limiting case when all observations are 0, i.e. $x_{(m)} = 0$, then eq. (34) implies that $\hat{b} = 0$ (the
 793 unbiased point estimate of b) which is expected since the density function goes to ∞ when
 794 $b \rightarrow 0$. In order to show that b^* is between the bounds for any sample x , we argue that b^*
 795 increases when any observation x_i increases without changing $x_{(m)}$. To do this, we rewrite
 796 eq. (33) as

$$G(x, b) = \sum_{i=1}^m \frac{1}{1 - x_i/b} - 2m = 0. \quad (35)$$

797 We see in eq. (35) that the function $G(x, b)$ is increasing with x_i and that it is decreasing
 798 with b . If $G(x, b) = 0$ for given x and b , then having $x'_i = x_i + \epsilon$, say, implies that $G(x', b) > 0$
 799 so we must have $b' < b$ in order for $G(x', b') = 0$. This monotonicity property of b^* thus
 800 implies that for any sample x there must be an increasing trajectory from the lower bound
 801 to the upper bound that goes through x . \square

802 The bounds provided by Proposition 5 can be used for initializing a search algorithm for
 803 solving eq. (33). They also imply that the MLE is strictly larger than $x_{(m)}$. However it is not
 804 obvious what is the expected value of b^* in general, although in the special case with $m = 1$
 805 it is equal to $2b/3$. Monte Carlo simulations indicate that b^* has a smaller variance than \hat{b}
 806 so that, even for small samples, the mean square error of b^* is slightly smaller than that of
 807 \hat{b} . But in practice the unbiased estimator \hat{b} seems attractive due to its ease of computation.
 808 However, the MLE computation might be justified when it saves the effort of obtaining a
 809 larger sample.

810 References

- 811 [1] Asmadi Ahmad, Ahmed El-Shafie, Siti Fatin Mohd Razali, and Zawawi Samba Mo-
 812 hamad. Reservoir optimization in water resources: a review. *Water Resources Manage-*
 813 *ment*, 28:3391–3405, 2014.

- 814 [2] A Alessandri, C Cervellera, D Maccio, and M Sanguineti. Optimization based on quasi-
815 Monte Carlo sampling to design state estimators for non-linear systems. *Optimization*,
816 59(7):963–984, 2010.
- 817 [3] Mohammad Abdullah Abid Almubaidin, Ali Najah Ahmed, Lariyah Bte Mohd Sidek,
818 and Ahmed Elshafie. Using metaheuristics algorithms (mhas) to optimize water supply
819 operation in reservoirs: a review. *Archives of Computational Methods in Engineering*,
820 29(6):3677–3711, 2022.
- 821 [4] Abdus Samad Azad, Md Shokor A Rahaman, Junzo Watada, Pandian Vasant, and Jose
822 Antonio Gamez Vintaned. Optimization of the hydropower energy generation using
823 meta-heuristic approaches: A review. *Energy Reports*, 6:2230–2248, 2020.
- 824 [5] Behrang Beiranvand and Parisa-Sadat Ashofteh. A systematic review of optimization
825 of dams reservoir operation using the meta-heuristic algorithms. *Water Resources Man-*
826 *agement*, pages 1–70, 2023.
- 827 [6] Richard Bellman. *Dynamic programming*. Princeton University Press, Princeton, NJ,
828 USA, 1958.
- 829 [7] Immanuel M Bomze and Gabriele Eichfelder. Copositivity detection by difference-of-
830 convex decomposition and ω -subdivision. *Mathematical Programming*, 138(1):365–400,
831 2013.
- 832 [8] BH Brito, EC Finardi, and FYK Takigawa. Mixed-integer nonseparable piecewise lin-
833 ear models for the hydropower production function in the unit commitment problem.
834 *Electric Power Systems Research*, 182:106234, 2020.
- 835 [9] P-L Carpentier, Michel Gendreau, and Fabian Bastin. Long-term management of a
836 hydroelectric multireservoir system under uncertainty using the progressive hedging
837 algorithm. *Water Resources Research*, 49(5):2812–2827, 2013.
- 838 [10] Pierre-Luc Carpentier, Michel Gendreau, and Fabian Bastin. Managing hydroelectric
839 reservoirs over an extended horizon using benders decomposition with a memory loss
840 assumption. *IEEE Transactions on Power Systems*, 30(2):563–572, 2014.

- 841 [11] Santiago Cerisola, Jesus M Latorre, and Andres Ramos. Stochastic dual dynamic pro-
842 gramming applied to nonconvex hydrothermal models. *European Journal of Operational*
843 *Research*, 218(3):687–697, 2012.
- 844 [12] Cristiano Cervellera, Mauro Gaggero, and Danilo Macciò. Lattice point sets for state
845 sampling in approximate dynamic programming. *Optimal Control Applications and*
846 *Methods*, 38(6):1193–1207, 2017.
- 847 [13] Cristiano Cervellera, Mauro Gaggero, Danilo Macciò, and Roberto Marcialis. Quasi-
848 random sampling for approximate dynamic programming. In *The 2013 International*
849 *Joint Conference on Neural Networks (IJCNN)*, pages 1–8. IEEE, 2013.
- 850 [14] Cristiano Cervellera and Marco Muselli. Efficient sampling in approximate dynamic
851 programming algorithms. *Computational Optimization and Applications*, 38(3):417–
852 443, 2007.
- 853 [15] Victoria CP Chen. Application of orthogonal arrays and mars to inventory forecasting
854 stochastic dynamic programs. *Computational Statistics & Data Analysis*, 30(3):317–341,
855 1999.
- 856 [16] Victoria CP Chen, David Ruppert, and Christine A Shoemaker. Applying experimental
857 design and regression splines to high-dimensional continuous-state stochastic dynamic
858 programming. *Operations Research*, 47(1):38–53, 1999.
- 859 [17] Ying Chen, Feng Liu, Jay M Rosenberger, Victoria CP Chen, Asama Kulvanitchaiya-
860 nunt, and Yuan Zhou. Efficient approximate dynamic programming based on design
861 and analysis of computer experiments for infinite-horizon optimization. *Computers &*
862 *Operations Research*, 124:105032, 2020.
- 863 [18] Ven Te Chow and Gonzalo Cortes-Rivera. Application of dddp in water resources plan-
864 ning. Technical report, University of Illinois at Urbana-Champaign. Water Resources
865 Center, 1974.

- 866 [19] Pascal Côté and Richard Arsenault. Efficient implementation of sampling stochastic dy-
867 namic programming algorithm for multireservoir management in the hydropower sector.
868 *Journal of Water Resources Planning and Management*, 145(4):05019005, 2019.
- 869 [20] Scott Davies. Multidimensional triangulation and interpolation for reinforcement learn-
870 ing. In *Advances in Neural Information Processing Systems*, pages 1005–1011, 1997.
- 871 [21] Vitor L De Matos, Andy B Philpott, and Erlon C Finardi. Improving the performance
872 of stochastic dual dynamic programming. *Journal of Computational and Applied Math-*
873 *ematics*, 290:196–208, 2015.
- 874 [22] Barnaby Dobson, Thorsten Wagener, and Francesca Pianosi. An argument-driven clas-
875 sification and comparison of reservoir operation optimization methods. *Advances in*
876 *Water Resources*, 128:74–86, 2019.
- 877 [23] Jitka Dupačová, Nicole Gröwe-Kuska, and Werner Römisch. Scenario reduction in
878 stochastic programming. *Mathematical Programming*, 95:493–511, 2003.
- 879 [24] Zhong-kai Feng, Wen-jing Niu, Chun-tian Cheng, and Sheng-li Liao. Hydropower system
880 operation optimization by discrete differential dynamic programming based on orthog-
881 onal experiment design. *Energy*, 126:720–732, 2017.
- 882 [25] Zhong-kai Feng, Wen-jing Niu, Zhi-qiang Jiang, Hui Qin, and Zhen-guo Song. Monthly
883 operation optimization of cascade hydropower reservoirs with dynamic programming
884 and Latin hypercube sampling for dimensionality reduction. *Water Resources Manage-*
885 *ment*, 34(6), 2020.
- 886 [26] Jean D. Gibbons. Estimation of the unknown upper limit of a uniform distribution.
887 *Sankhya: The Indian Journal of Statistics, Series B (1960-2002)*, 36(1):29–40, 1974.
- 888 [27] Albertas Gimbutas and Antanas Žilinskas. An algorithm of simplicial Lipschitz opti-
889 mization with the bi-criteria selection of simplices for the bi-section. *Journal of Global*
890 *Optimization*, 71(1):115–127, 2018.

- 891 [28] Raphael EC Gonçalves, Erlon Cristian Finardi, and Edson Luiz da Silva. Applying
892 different decomposition schemes using the progressive hedging algorithm to the oper-
893 ation planning problem of a hydrothermal system. *Electric power Systems Research*,
894 83(1):19–27, 2012.
- 895 [29] Quentin Goor, R Kelman, and Amaury Tilmant. Optimal multipurpose-multireservoir
896 operation model with variable productivity of hydropower plants. *Journal of Water
897 Resources Planning and Management*, 137(3):258–267, 2011.
- 898 [30] LCGJM Habets, Pieter J Collins, and Jan H van Schuppen. Reachability and con-
899 trol synthesis for piecewise-affine hybrid systems on simplices. *IEEE Transactions on
900 Automatic Control*, 51(6):938–948, 2006.
- 901 [31] Tito Homem-de Mello, Vitor L De Matos, and Erlon C Finardi. Sampling strategies and
902 stopping criteria for stochastic dual dynamic programming: a case study in long-term
903 hydrothermal scheduling. *Energy Systems*, 2(1):1–31, 2011.
- 904 [32] Reiner Horst. An algorithm for nonconvex programming problems. *Mathematical Pro-
905 gramming*, 10(1):312–321, 1976.
- 906 [33] Sharon A Johnson, Jerry R Stedinger, Christine A Shoemaker, Ying Li, and Jose Alberto
907 Tejada-Guibert. Numerical solution of continuous-state dynamic programs using linear
908 and spline interpolation. *Operations Research*, 41(3):484–500, 1993.
- 909 [34] Kartlos J Kachiashvili and Alexander L Topchishvili. Parameters estimators of irreg-
910 ular right-angled triangular distribution. *Model Assisted Statistics and Applications*,
911 11(2):179–184, 2016.
- 912 [35] John W Labadie. Optimal operation of multireservoir systems: State-of-the-art review.
913 *Journal of Water Resources Planning and Management*, 130(2):93–111, 2004.
- 914 [36] Bernard F Lamond and Luckny Zéphyr. Note on “Parameters estimators of irregular
915 right-angled triangular distribution”. *Model Assisted Statistics and Applications*, 16(4),
916 2021. To appear.

- 917 [37] Douglas W Moore. Simplicial mesh generation with applications. Technical report,
918 Cornell University, 1992.
- 919 [38] Mojtaba Moravej and Seyed-Mohammad Hosseini-Moghari. Large scale reservoirs sys-
920 tem operation optimization: the interior search algorithm (isa) approach. *Water Re-*
921 *sources Management*, 30:3389–3407, 2016.
- 922 [39] José L Morillo, Juan F Pérez, Luckny Zéphyr, C Lindsay Anderson, and Angela Ca-
923 dena. Assessing the impact of wind variability on the long-term operation of a hydro-
924 dominated system. In *2017 IEEE PES Innovative Smart Grid Technologies Conference*
925 *Europe (ISGT-Europe)*, pages 1–6. IEEE, 2017.
- 926 [40] José L Morillo, Luckny Zéphyr, Juan F Pérez, C Lindsay Anderson, and Ángela Cadena.
927 Risk-averse stochastic dual dynamic programming approach for the operation of a hydro-
928 dominated power system in the presence of wind uncertainty. *International Journal of*
929 *Electrical Power & Energy Systems*, 115:105469, 2020.
- 930 [41] Rémi Munos and Andrew Moore. Variable resolution discretization in optimal control.
931 *Machine Learning*, 49(2-3):291–323, 2002.
- 932 [42] Daniel M Murray and Sidney J Yakowitz. Constrained differential dynamic pro-
933 gramming and its application to multireservoir control. *Water Resources Research*,
934 15(5):1017–1027, 1979.
- 935 [43] Nay Myo Lin, Xin Tian, Martine Rutten, Edo Abraham, José M Maestre, and Nick
936 van de Giesen. Multi-objective model predictive control for real-time operation of a
937 multi-reservoir system. *Water*, 12(7):1898, 2020.
- 938 [44] Kristian Nolde, Markus Uhr, and Manfred Morari. Medium term scheduling of a hydro-
939 thermal system using stochastic model predictive control. *Automatica*, 44(6):1585–1594,
940 2008.
- 941 [45] Remigijus Paulavičius and Julius Žilinskas. Global optimization using the branch-and-
942 bound algorithm with a combination of Lipschitz bounds over simplices. *Technological*
943 *and Economic Development of Economy*, 15(2):310–325, 2009.

- 944 [46] Remigijus Paulavičius and Julius Žilinskas. *Simplicial Global Optimization*. Springer,
945 2014.
- 946 [47] Mario VF Pereira. Optimal stochastic operations scheduling of large hydroelectric sys-
947 tems. *International Journal of Electrical Power & Energy Systems*, 11(3):161–169, 1989.
- 948 [48] Mario VF Pereira and Leontina MVG Pinto. Multi-stage stochastic optimization applied
949 to energy planning. *Mathematical programming*, 52(1):359–375, 1991.
- 950 [49] MVF Pereira and LMVG Pinto. Stochastic optimization of a multireservoir hydroelectric
951 system: A decomposition approach. *Water resources research*, 21(6):779–792, 1985.
- 952 [50] Deepti Rani and Maria Madalena Moreira. Simulation–optimization modeling: a survey
953 and potential application in reservoir systems operation. *Water Resources Management*,
954 24:1107–1138, 2010.
- 955 [51] Luciano Raso and Pierre Olivier Malaterre. Combining short-term and long-term reser-
956 voir operation using infinite horizon model predictive control. *Journal of Irrigation and*
957 *Drainage Engineering*, 143(3):B4016002, 2017.
- 958 [52] Steffen Rebennack. Combining sampling-based and scenario-based nested benders de-
959 composition methods: application to stochastic dual dynamic programming. *Mathe-*
960 *matical Programming*, 156:343–389, 2016.
- 961 [53] Andrzej Ruszczyński and Alexander Shapiro. Stochastic programming models. *Hand-*
962 *books in Operations Research and Management Science*, 10:1–64, 2003.
- 963 [54] Antonio Sala and Leopoldo Armesto. Adaptive polyhedral meshing for approximate
964 dynamic programming in control. *Engineering Applications of Artificial Intelligence*,
965 107:104515, 2022.
- 966 [55] Alexander Shapiro, Darinka Dentcheva, and Andrzej Ruszczyński. *Lectures on stochas-*
967 *tic programming: modeling and theory*. SIAM, 2009.
- 968 [56] Hoang Tuy. Effect of the subdivision strategy on convergence and efficiency of some
969 global optimization algorithms. *Journal of Global Optimization*, 1(1):23–36, 1991.

- 970 [57] Gökçen Uysal, Dirk Schwanenberg, Rodolfo Alvarado-Montero, and Aynur Şensoy. Short
971 term optimal operation of water supply reservoir under flood control stress using model
972 predictive control. *Water Resources Management*, 32:583–597, 2018.
- 973 [58] Wim van Ackooij, René Henrion, Andris Möller, and Riadh Zorgati. Joint chance con-
974 strained programming for hydro reservoir management. *Optimization and Engineering*,
975 15(2):509–531, 2014.
- 976 [59] Bin Xu, Ping-An Zhong, Renato C Zambon, Yunfa Zhao, and William W-G Yeh. Sce-
977 nario tree reduction in stochastic programming with recourse for hydropower operations.
978 *Water Resources Research*, 51(8):6359–6380, 2015.
- 979 [60] Dmitry S Yershov and Steven M LaValle. Simplicial Dijkstra and A* algorithms: From
980 graphs to continuous spaces. *Advanced Robotics*, 26(17):2065–2085, 2012.
- 981 [61] Luckny Zéphyr and C Lindsay Anderson. Stochastic dynamic programming approach
982 to managing power system uncertainty with distributed storage. *Computational Man-
983 agement Science*, 15(1):87–110, 2018.
- 984 [62] Luckny Zéphyr, Pascal Lang, and Bernard F Lamond. Adaptive monitoring of the pro-
985 gressive hedging penalty for reservoir systems management. *Energy Systems*, 5(2):307–
986 322, 2014.
- 987 [63] Luckny Zéphyr, Pascal Lang, and Bernard F Lamond. Controlled approximation of the
988 value function in stochastic dynamic programming for multi-reservoir systems. *Compu-
989 tational Management Science*, 12(4):539–557, 2015.
- 990 [64] Luckny Zéphyr, Pascal Lang, Bernard F Lamond, and Pascal Côté. Controlled ap-
991 proximation of the stochastic dynamic programming value function for multi-reservoir
992 systems. In *Computational Management Science*, pages 31–37. Springer, 2016.
- 993 [65] Luckny Zéphyr, Pascal Lang, Bernard F Lamond, and Pascal Côté. Approximate
994 stochastic dynamic programming for hydroelectric production planning. *European Jour-
995 nal of Operational Research*, 262(2):586–601, 2017.

996 [66] A Žilinskas and J Žilinskas. Global optimization based on a statistical model and
997 simplicial partitioning. *Computers & Mathematics with Applications*, 44(7):957–967,
998 2002.